CAPITAL UNIVERSITY OF SCIENCE AND TECHNOLOGY, ISLAMABAD


# High Gain FSS-based Aperture Coupled Patch Antenna Array for X-band Satellite Applications

by

Raz Muhammad

A thesis submitted in partial fulfillment for the degree of Master of Science

in the

Faculty of Engineering
Department of Electrical Engineering

2022

*Dedicated to my family*


# CERTIFICATE OF APPROVAL

## High Gain FSS-based Aperture Coupled Patch Antenna Array for X-band Satellite Applications

by

Raz Muhammad

(MEE173027)

### THESIS EXAMINING COMMITTEE

| S. No. | Examiner | Name | Organization |
|---|---|---|---|
| (a) | External Examiner | Dr. Qaisar Abbas Naqvi | QAU, Islamabad |
| (b) | Internal Examiner | Dr. Muhammad Riaz | CUST, Islamabad |
| (c) | Supervisor | Dr. Noor Muhammad Khan | CUST, Islamabad |

Dr. Noor Muhammad Khan
Thesis Supervisor
December, 2022

Dr. Noor Muhammad Khan
Head
Dept. of Electrical Engineering
December, 2022

Dr. Imtiaz Ahmad Taj
Dean
Faculty of Engineering
December, 2022

# *Author's Declaration*

I, **Raz Muhammad** hereby state that my MS thesis titled "**High Gain FSS-based Aperture Coupled Patch Antenna Array for X-band Satellite Applications**" is my own work and has not been submitted previously by me for taking any degree from Capital University of Science and Technology, Islamabad or anywhere else in the country/abroad.

At any time if my statement is found to be incorrect even after my graduation, the University has the right to withdraw my MS Degree.

**(Raz Muhammad)**

Registration No: MEE173027

# *Plagiarism Undertaking*

I solemnly declare that research work presented in this thesis titled "**High Gain FSS-based Aperture Coupled Patch Antenna Array for X-band Satellite Applications**" is solely my research work with no significant contribution from any other person. Small contribution/help wherever taken has been duly acknowledged and that complete thesis has been written by me.

I understand the zero tolerance policy of the HEC and Capital University of Science and Technology towards plagiarism. Therefore, I as an author of the above titled thesis declare that no portion of my thesis has been plagiarized and any material used as reference is properly referred/cited.

I undertake that if I am found guilty of any formal plagiarism in the above titled thesis even after award of MS Degree, the University reserves the right to withdraw/revoke my MS degree and that HEC and the University have the right to publish my name on the HEC/University website on which names of students are placed who submitted plagiarized work.

**(Raz Muhammad)**
Registration No: MEE173027

# *Acknowledgement*

I humbly praise and grateful to **ALMIGHTY ALLAH**, Who permits me to live and accomplish tasks, including the research work presented in this thesis.

I would like to express my gratitude to my advisor **Prof. Dr. Noor Muhammad Khan**, Head of Electrical Engineering Department, Capital University of Science and Technology (CUST), Islamabad, for his support, encouragement, and mentorship. I would like to thank him because of the opportunity he has given me to follow and fulfill my research interests. I am so grateful for what I have learned from his gracious personality.

I am thankful to the administration of CUST for providing me with an excellent environment perfect for conducting research. I am also thankful to Dean, Faculty of Engineering, **Prof. Dr. Imtiaz Ahmad Taj**.

I also wish to express my feelings of gratitude to my family, who prayed for my health and brilliant future. I would not have achieved these goals without their sincere co-operation and love. I am also using this opportunity to thank all my friends who prayed for me and encouraged me through their love and sincerity.

**(Raz Muhammad)**

# *Abstract*

For satellite and radar applications, high-gain antennas are required. This demand can be fulfilled with the help of antenna arrays. But adding more array elements results a larger array size. One of the solutions to increasing the gain of any antenna is to utilize reflective surfaces such as frequency selective surfaces (FSSs). By utilizing FSS, one can increase the gain of an antenna or antenna array while maintaining a compact size. In this thesis, a design of a high-gain FSS-based aperture coupled patch array antenna is presented for X-band satellite communication applications. Initally, a single element of an aperture coupled patch is designed and optimized to get response at the center frequency of 10 GHz. In the second step, a 1×4 linear antenna array of the proposed aperture coupled patch antenna is designed to achieve high gain for the frequency band of interest. For the feeding of array elements, a conventional 1×4 corporate feeding network is designed. It is observed that the antenna array offers wide impedane bandwidth and high gain of 8.9 dBi with low sidelobe levels (SLLs) of 14.5 dB. To further enhance the gain, an array of FSS is utilized and placed beneath the array antenna. The FSS design consists of a modified square-loop element and it is designed to operate at 10 GHz. The utilization of the FSS reflector tends to achieve 11.2 dBi peak gain and also reduce the SLLs by 2 dB. From the presented results, one can observe that the designed FSS-based array can be utilized in satellite communication applications.

# Contents

# List of Figures

# List of Tables

# Abbreviations

| | |
|---|---|
| **3D** | Three-dimensional |
| **5G** | Fifth-generation |
| **AESA** | Active Electronic Scan Array |
| **AF** | Array Factor |
| **AR** | Axial Ratio |
| **BER** | Bit-error Rate |
| **DD** | Dense Dielectric |
| **EMI** | Electromagnetic Interference |
| **FSS** | Frequency Selective Surface |
| **HPBW** | Half Power Beamwidth |
| **MMIC** | Microwave Monolithic Integrated Circuit |
| **mmwave** | Millimeter-wave |
| **NFC** | Near-field Communication |
| **PCB** | Printed Circuit Board |
| **PESA** | Passive Electronic Scan Array |
| **PRS** | Partially Reflective Surface |
| **RCS** | Radar Cross-section |
| **RF** | Radio Frequency |
| **RFID** | Radio Frequency Identification |
| **SISL** | Substrate Integrated Suspended Line |
| **SLL** | Sidelobe Level |
| **TV** | Television |
| **UWB** | Ultra Wideband |
| **WiFi** | Wireless Fidelity |

**WiMAX** Worldwide Interoperability for Microwave Access

**WLAN** Wireless Local Area Network

# Chapter 1

# Introduction

This chapter provides a brief historical background as well as the essence of antennas in communication systems. Antenna arrays, microstrip patch array structure and performance, and Frequency Selective Surfaces (FSSs) are covered before outlining the research objective. The research objective is discussed after summing up the preceding related topics. A brief outline of the thesis is provided at the end.

## 1.1 Background

An antenna is the most crucial component of every communication system that allows engineers and scientists to send radio signals wirelessly using electromagnetic waves. Heinrich Hertz first discovered electromagnetic waves in 1886 [1]. Hertz created an antenna to demonstrate British mathematician and physicist James Clerk Maxwell's hypothesis that electromagnetic radiation is just one example of a larger class of electromagnetic phenomena that can travel through air (or empty space) as waves. Hertz demonstrated it with a dipole transmitter that generated sparks that were received on the ends of a copper ring located at a specific distance from the transmitter.

Guglielmo Marconi, the inventor of radio telegraphy, created various antennas for wireless communication signals and realized the need of tall antenna systems in conveying low-frequency signals. The operating frequencies of early antennas, such as those designed by Marconi and others, were determined primarily by antenna size and shape. An oscillator was used in later antennas to adjust the frequency, which generated the transmitted signal. Modulation became possible in the early half of the 19th century with the invention of vacuum tubes and triodes, among other electrical and microwave devices. These breakthroughs make it possible to use communication technology to develop a modern society. As technology has advanced, a variety of effective antennas have been exploited for several applications. A few of them include cellular communication systems, Radio Frequency Identification (RFID), Near-field Communication (NFC), and wireless communication.

Radio frequency (RF) internet systems have been developed, such as Worldwide Interoperability for Microwave Access (WiMAX) and Wireless Local Area Network (WLAN) devices. In addition, antennas have been a critical component of radar and satellite communication. Following World War-II, Dr. Clark proposed in his well-known research paper "wireless world" in 1945 that three satellites spaced at a 120-degree angle could be used to cover the entire planet. In later works, he also discussed the projected space station. His contributions laid the foundation for satellite communication, an essential component of daily life that enables people to receive television (TV) and radio broadcasts and maintain essential communications in remote places, both on land and sea, for civilian and military use [2].

Satellites are now employed to do more precise global positioning and navigation, as well as climate and environmental forecasting. According to [3], big-sized antennas produce high gain that is essential to amplify signals for communication and radar applications. Randy L. Haupt discussed two candidates for highly efficient antenna applications: reflectors and arrays. Reflectors are huge structures and are inexpensive, but they consists of complicated mechanisms to track the signals for satellites. Due to this shortcoming, array antennas are a better solution because of

their wide scanning with static antennas, fast movement, ability for beam forming, and ability for low cross section.

Antenna arrays have a nearly century-long history and have developed alongside the advancement of electronic and information technology, playing a pivotal role in radar and wireless communications. An interconnected group of interconnecting antennas used to send or receive electromagnetic radiation is collectively termed an antenna array. The very first antenna array was devised more than a century ago, in the 1900s, when Nobel Prize-winning Ferdinand Braun combined three monopoles in a triangular pattern to generate a cardioids radiation pattern [4]. Array antennas, according to Xiao, were first utilized for applications related to radar, but as processing technology evolved, beam forming applications were adopted, which use antenna arrays for scanning and are more flexible than mechanical scanning. Bell Laboratories used a smart antenna, or adaptive array antenna, for satellite communication in the 1970s to demonstrate scanning spot beams. As mobile communication advanced, adaptive antennas were later employed in cellular communication technology [5].

In contrast to the demands of modern RF and microelectronic technology, increasing the number of array elements also increases the total size of the array or system. Utilizing FSSs is a more recent research area that can improve array performance. To improve bandwidth, gain, and directivity while lowering radar cross section, surface wave, and sidelobes, FSSs have been used on antennas and antenna arrays [6]. The following sections of this chapter will go into greater detail about array antennas, microstrip antennas and arrays, and frequency selective surfaces.

## 1.2 Antenna Arrays

When Guglielmo Marconi conducted the ground-breaking transcontinental wireless communication experiment in December 1901, he was the first to employ arrays as the transmitting antenna [7]. The goal of this effort was to demonstrate a wireless system capable of transmitting high-power Morse codes. Copper wires

were suspended from a triangular stay that was stretched between the masts. The aerial was made into a fan shape by being a yard apart at the top and merging at the bottom, as shown in Fig. 1.1.

FIGURE 1.1: The first cone aerial array [8].

An antenna array is defined as a radiating element formed by placing different individual antennas in an electrical and geometrical pattern (phase and distance). The term "antenna element" refers to each individual antenna that makes up a multi-element array. Any type of antenna, including apertures, dipoles, microstrips, loops, reflectors, and horns, can be used as array elements. Although the radiation pattern of single element is typically relatively broad and each one has low gain (directivity), large single antennas potentially have high gain and directivity characteristics. Highly directional characteristics can be achieved by increasing the number of individual antenna elements in a multi-element array. If the current flowing through each element is the same and mutual coupling is ignored, the vector summation of the fields that each element radiates defines the overall field pattern. Therefore, constructive interference offers strong directivity in the desired direction, while destructive interface cancels out in all other directions.

The entire geometrical structure of the array, the excitation amplitude, phase, inter-element spacing, and the relative shape of each individual element are the main factors that can be manipulated to control the overall radiation characteristics of an array antenna [9].

### 1.2.1 Types of Antenna Arrays

According to geometrical arrangement, arrays are fundamentally categorized as:

- Linear array
- Planar array
- Circular array

#### 1.2.1.1 Linear Array

A linear array is one of the simplest array configuration. In linear array, the antenna elements are arranged along a straight line, as shown in Fig. 1.2. The major lobes of the array are formed and guided into a single beam by a linear phase taper of the signal provided to the array components. The field produced by a single antenna element at the origin multiplied by the array factor (AF) results in the total field of the array. The general far-field pattern of an N-element linear array is described by Eq. (1.1).

$$f(\theta, \phi) = E_n(\theta, \phi) \times \mathrm{AF}_n(\theta, \phi) \tag{1.1}$$

where

$$\mathrm{AF} = \sum_{n=1}^{N} e^{-j(n-1)\psi} \tag{1.2}$$

where, $\psi = kd\cos(\theta) + \beta$, where $\beta$ is a relative phase between elements, and $d$ denotes the distance between the array elements [9]. It implies from Eq. (1.2) that the relative phase between the elements can be used to control the AFs of uniform linear arrays. A uniform array is one that contains elements of the same kind, excitation, and progressive phase.

There are two configurations of linear arrays with respect to the radiated field direction.

- Broadside array

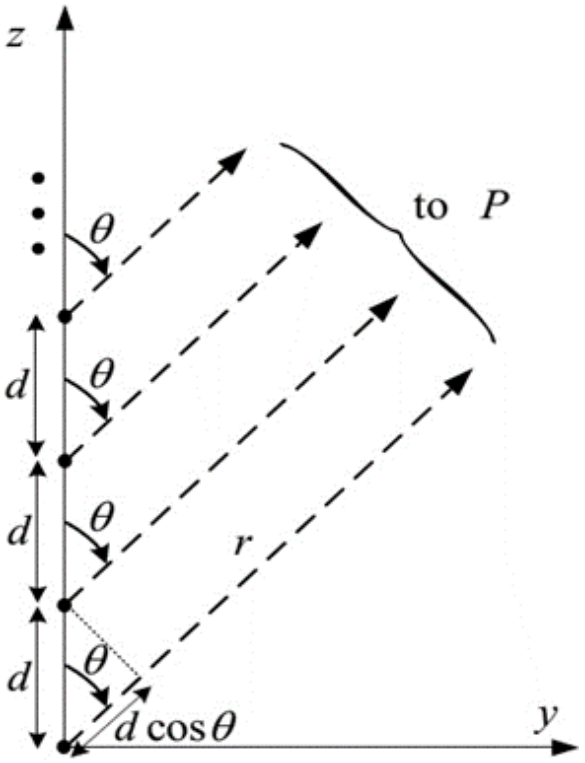


FIGURE 1.2: Linear array with N-elements that have uniform excitation amplitude and spacing [9].

- End-fire array

**1.2.1.1.1 Broadside Array** In a broadside array, the components are arranged next to each other and orthogonal to the array axis. The primary lobe direction of this type of array arrangement is perpendicular to the array axis, as shown in Fig. 1.3. Elements are uniformly distributed and fed with equal amplitude and phase current [9, 10].

Depending on the desired beamwidth, a number of equal-sized dipoles are used. All dipoles are fed with signals of the same phase. A broadside array can enhance the gain and directivity when combined with a reflector, and this also becomes unidirectional. The same array can be employed behind it at a distance of $\lambda/4$ fed with current having a phase shift of 90 degrees [9, 10].

**1.2.1.1.2 End-fire Array** As was previously explained, from the perspective of the layout of elements, the end-fire array and the broadside array are very similar.

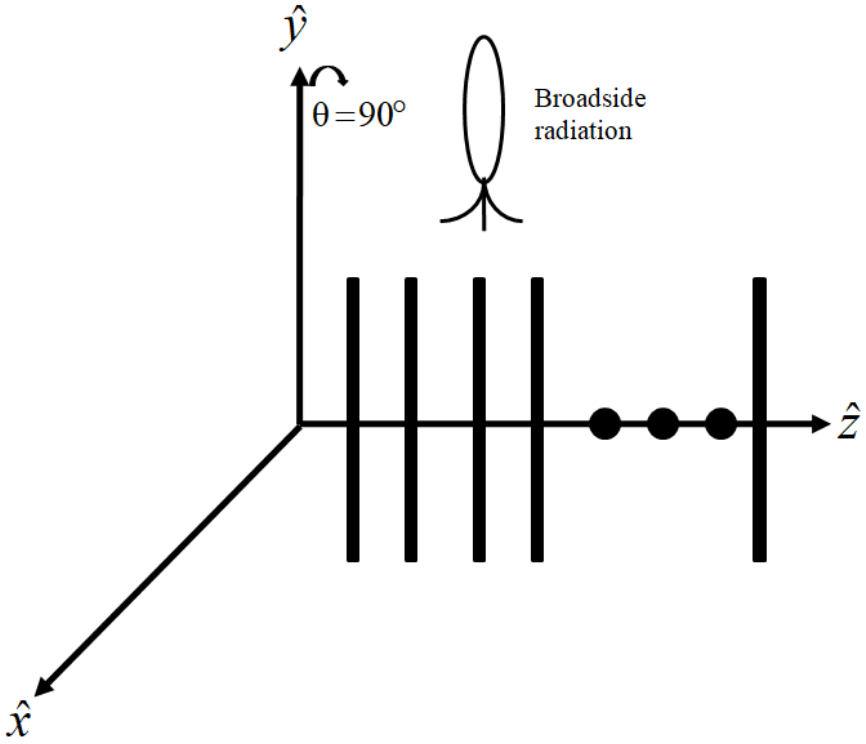


FIGURE 1.3: Broadside array radiation and orientation [11].

The difference lies in the radiation's main lobe direction. In the end-fire array, it is parallel to the axis of the antenna array as shown in Fig. 1.4. In the end-fire array, an equal number of identical antennas are arranged along a line.

Each element is provided directly with similar currents on an individual basis, but as the arrangement advances, the phases of the currents subsequently change, making the entire array arrangement unidirectional. The field direction of the principle lobe is along the axis of the array [9, 10].

#### 1.2.1.2 Planar Array

Planar arrays are formed when elements of an array are organized in a plane rather than along a single axis, as shown in Fig. 1.5. In comparison to the low directivity of each individual element, planar arrays offer directional beams, symmetrical patterns with minimum sidelobes, and high directivity (narrow beam width). The beam can be pointed in any direction, as shown in Fig. 1.5 [12]. The $y$-axis has N arrays evenly spaced apart, and the $x$-axis has M arrays. If the current distribution

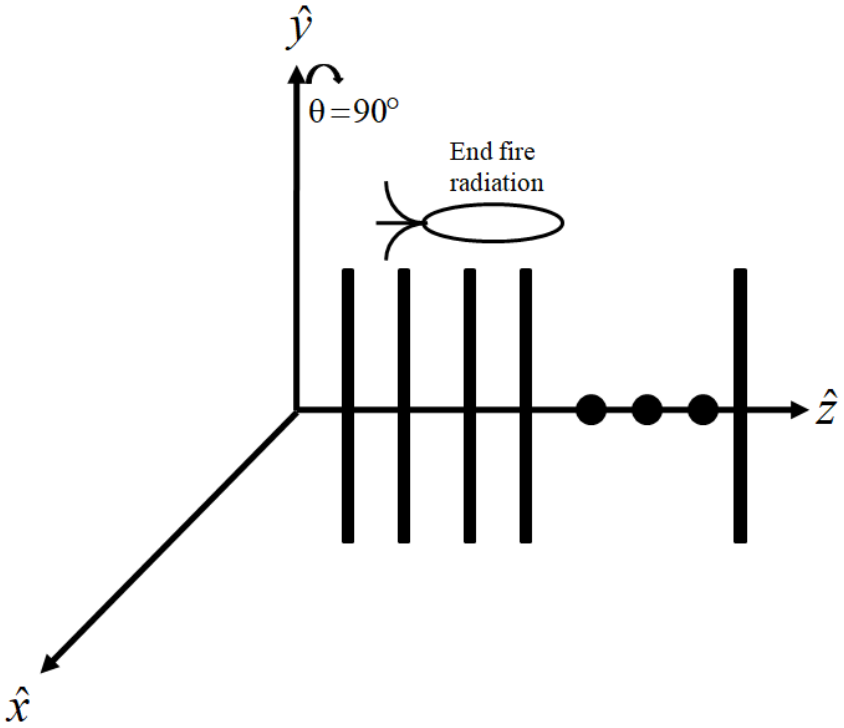


FIGURE 1.4: End-fire array radiation and orientation [11].

along each axis is assumed to be the same, then the normalized AF can be written as [12]:

$$\mathrm{AF}\,(\theta,\phi) = \left[\frac{1}{M}.\frac{\sin\left(M.\frac{\psi_x}{2}\right)}{\sin\left(\frac{\psi_x}{2}\right)}\right] \times \left[\frac{1}{N}.\frac{\sin\left(N.\frac{\psi_y}{2}\right)}{\sin\left(\frac{\psi_y}{2}\right)}\right] \tag{1.3}$$

where

$$\psi_x = d_x \cos\theta \sin\phi + \beta_x \tag{1.4}$$

and

$$\psi_y = d_y \cos\theta \sin\phi + \beta_y \tag{1.5}$$

The element spacing, phase shift, frequency, and elevation angle all determine the linear phase functions . The main lobe is directed by the phase shift ($\beta_x$ and $\beta_y$) of the inter-elements, whereas the beamwidth and sidelobe level (SLL) are determined by the amplitude distribution and inter-elements spacing. Greater sidelobes and smaller main lobe width result from an increase in inter-element

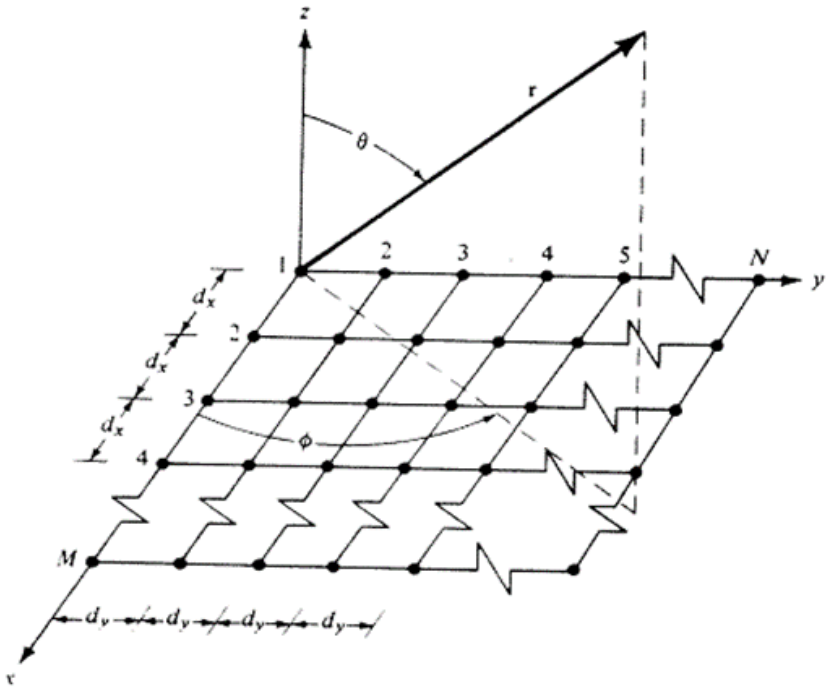


FIGURE 1.5: N×M planar array structure distributed in $xy$ plane [12].

spacing value. Directivity can also be increased by increasing antenna elements [13].

#### 1.2.1.3 Circular Array

The circular array is a type of planar configuration in which the radiating elements are spread in a circular pattern, as seen in Fig. 1.6. There are no edge elements in circular arrays. A circular array's beam pattern can be electronically rotated without any edge limitations. The AF of the circular array is given by the following equation [9]:

$$\mathrm{AF} = \sum_{n=1}^{N} I_n e^{-jka(\cos\psi_n - \cos\psi_{0n})} \tag{1.6}$$

where

$$\psi_n = \cos^{-1}\left[\sin\theta\cos\left(\phi - \phi_n\right)\right] \tag{1.7}$$

and

$$\psi_{0n} = \cos^{-1}\left[\sin\theta_0\cos\left(\phi_0 - \phi_n\right)\right] \tag{1.8}$$

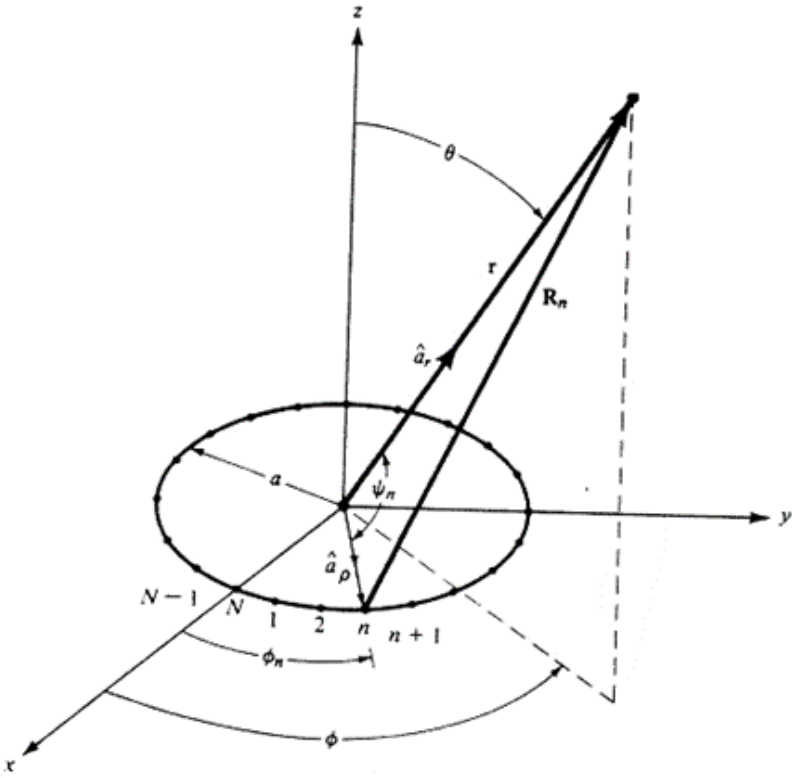


FIGURE 1.6: Circular array structure [9].

### 1.2.2 Applications of Arrays

Antenna arrays in mobile communications systems have successfully solved the problem of restricted channel capacity and the growing requirement for a substantial quantity of mobiles on allocated frequency channels in recent years. Numerous studies have shown that an array may improve channel capacity and spectrum efficiency in mobile communications systems, expand range coverage, personalize beamforming, steer multiple beams to track multiple mobiles, and electronically compensate for aperture distortion. Additionally, it reduces bit-error rate (BER), co-channel interferences, system complexity, and multipath fading. The development of a high-capacity communications system has been claimed to be dependent on smart antennas and the algorithms that control them. In the research field, array design for mobile communications, numerous prototypes have been built, evaluated, tested, and employed [14].

Beamforming, in which a wireless signal is concentrated on a specific receiving device, is an illustration of RF management. A number of technologies, including

radar, sonar, wireless communications, and acoustics, employ beamforming. The RF management technology directs radio and sound waves for signal transmission or reception. The traditional technique of beam pointing or beam shaping may point a beam in the desired direction by simply changing the phase of signals that are transmitted from various elements. Gain of each signal is maintained at the same level. It establishes the array's overall gain in the direction known as the beam scanning direction or range. Since the geometry of the antenna pattern is fixed in this case, the position of the sidelobes with respect to the main beam and their level remain unchanged. Alternatively it is added that, even if the main beam is directed towards different angles with the adjustment of individual phases, the sidelobes positions in relation to the main lobe remain constant. By modifying the gain and phase of each element, this may be altered. Modern radars, called phased arrays, are utilized in a wide range of military and civilian applications on the ground, in the air, and even in space. There are two common types of phased array radars, such as Passive Electronic Scan Array (PESA) and Active Electronic Scan Array (AESA). Nevertheless, PESA is among the most widely used alternatives to AESA, hybrid beam forming phased arrays, and digital beam forming. The antenna parts of a PESA are coupled to a single transmitter and/or receiver [15]. The term active phased array, also known as active electronically scanned array, refers to a phased array in which each antenna element includes a digital transmitter and receiver that produces the phase shift to electronically steer the main beam of antenna. Second-generation phased-array technology that is more recent and employed for military applications is called active arrays. They may concurrently produce a number of radio wave beams at multiple frequencies and in diverse orientations, unlike PESAs (elevation and azimuth planes).

## 1.3 Microstrip Patch Antenna Array

Microstrip antennas are extensively used as single elements and in arrays in the communication industry. To accomplish some radiation parameters that cannot be obtained with a single antenna element, we can use an approach that involves

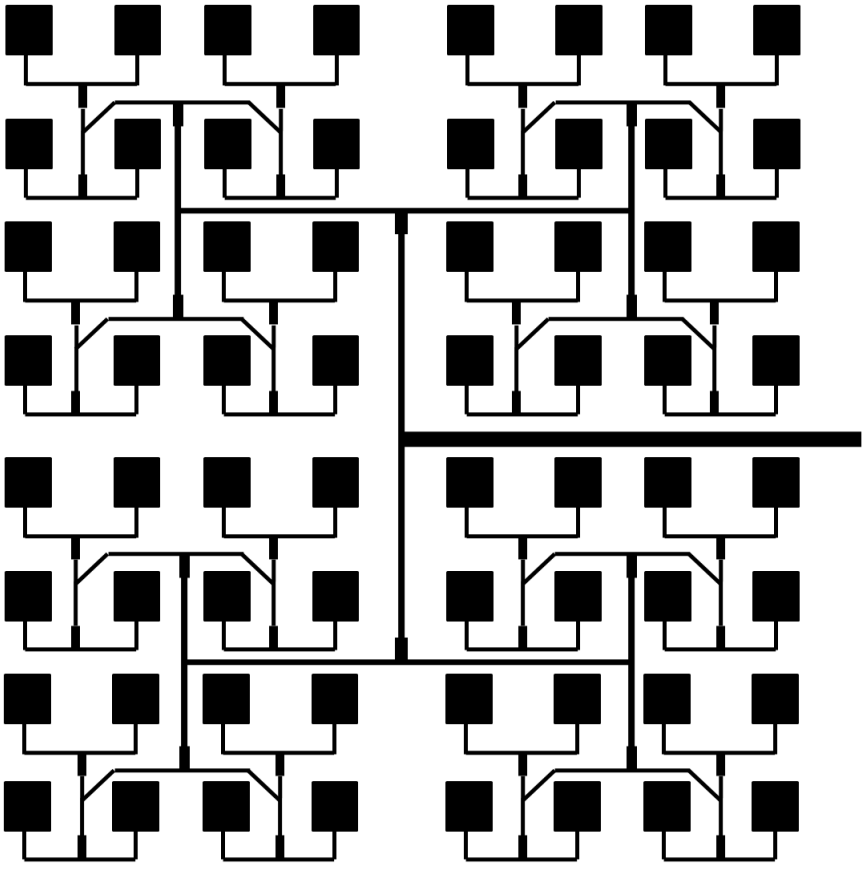

FIGURE 1.7: Design of microstrip patch antenna array [17].

combining radiating elements together in a geometric and electrical arrangement termed as antenna array. Different types of arrays have been discussed in Section 1.2; in practical applications, the type of array is often chosen based on required performance. However, the majority of large phased array applications use planar array configurations [16]. Planar microstrip arrays can be used to form a pencil beam, and there are different techniques to feed the array elements. An array of 8×8 elements with a corporate feed network is shown in Fig. 1.7. Major lobe direction can be pointed in any direction using phase shift as described in Eq. (1.3).

### 1.3.1 Design of Microstrip Patch Antenna

An elementary microstrip patch antenna has a ground plane on one side of a dielectric substrate and a metallic patch on the other. In general, metal is a

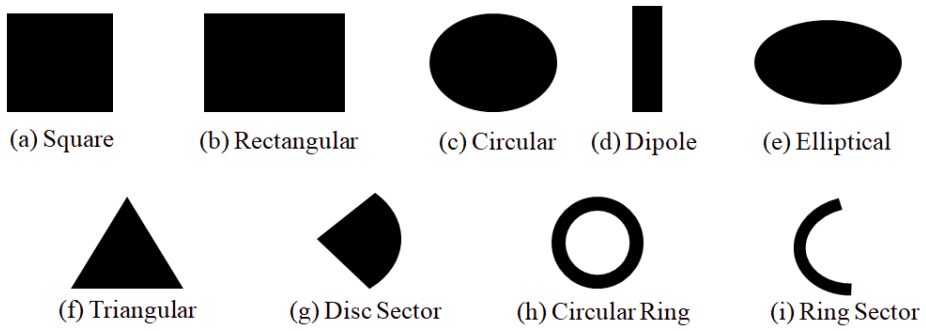


FIGURE 1.8: Basic shapes of patch antenna [9].

radiating element. It is a suitable printed resonant antenna for semi-hemispheric coverage narrow-band microwave wireless communications. To make analysis and performance evaluation simple, patches are typically elliptical square, triangular, circular, rectangular, square, or another similar shape, as shown in Fig. 1.8. Rectangular and circular patches are the most fundamental and commonly used microstrip antennas. An effective antenna is required for both the simplest and most sophisticated applications. Most wireless systems, including cellular, WiFi, wireless telephony, radar, and satellite communication systems, use microstrip patch antennas due to their simplicity of integration with microwave monolithic integrated circuits (MMICs). The simplest technique is the feed line method to feed excitation current to the patch. It is a microstrip line directly connected to a radiating patch whose impedance is matched to the RF source impedance. Although microstrip antennas come in a broad variety of configurations, there are generally four essential parts to any antenna, as shown in Fig. 1.9 [9, 18].

The geometry of a single microstrip patch antenna is shown in Fig. 1.9, where $W$ denotes the patch's width, $L$ denotes its length, $d$ denotes the substrate's height, and $\epsilon_r$ denotes the substrate's dielectric constant.

The relative permittivity, which measures an insulator's capability to store electric energy in an electromagnetic field, is the ratio of a substrate or medium's permittivity to that of vacuum. Relative permittivity $\epsilon_r$ also sometimes called as dielectric constant has a defined value for various materials, with vacuum having a value of 1. However, Effective permittivity $\epsilon_{reff}$ must be explained in order

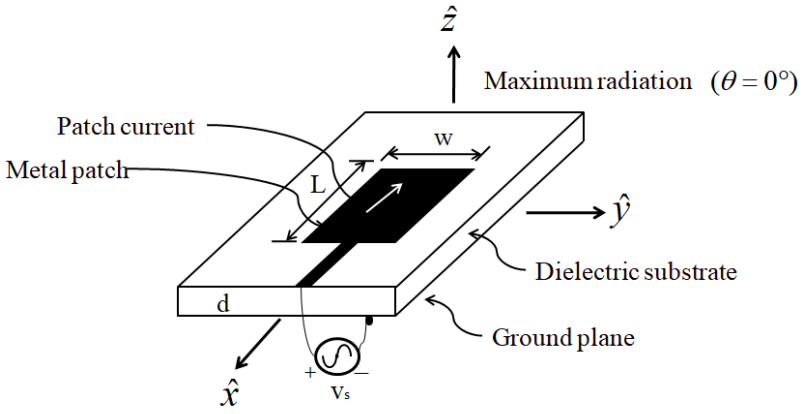


FIGURE 1.9: Geometry of microstrip patch antenna [19].

to comprehend the dynamics of microstrip line propagation. When it comes to microstrip transmission lines or microstrip patch antennas, electromagnetic fields to some extent inhabit in the atmosphere and in the dielectric between the strip conductor and the ground. The effective permittivity is influenced by substrate thickness $d$ and conductor width $W$ [20].

Due to their low production costs, microstrip antennas are capable of being made in large quantities. It has been easily incorporated using microwave integrated circuits. It can accommodate both circular and linear polarization. It is less expensive, lightweight, and small in size. Microstrip antennas are robust mechanically when mounted on a rigid surface. It has some limitations nevertheless, and a complicated design is needed to address them. It has a narrow bandwidth and a low threshold tolerance. It has a large ohmic loss in the array feed network. The majority of microstrip antennas emit into half space, and surface waves are excited. Numerous strategies, such as probe-fed antennas, patch antennas with thick substrates electrically, stacked shorted patches, and slotted patch antennas, have been suggested and researched to get around the fundamental constraint.

To determine the patch radiator's $W$ and $L$, following equationas can be used [9].

$$W = \frac{c}{2f_r}\left(\frac{\epsilon_r + 1}{2}\right)^{\frac{-1}{2}} \tag{1.9}$$

$$L = L_{eff} - 2\Delta L \tag{1.10}$$

where

$$L_{eff} = \frac{c}{2f_r\sqrt{\epsilon_r}} \tag{1.11}$$

and

$$\Delta L = 0.412 \times d \left[ \frac{(\epsilon_{reff} + 0.3)\left(\frac{W}{d} + 0.264\right)}{(\epsilon_{reff} - 0.258)\left(\frac{W}{d} + 0.8\right)} \right] \tag{1.12}$$

where

$$\epsilon_{reff} = \frac{\epsilon_r + 1}{2} \times \frac{\epsilon_r - 1}{2} \left(1 + 12\frac{d}{W}\right)^{\frac{-1}{2}} \tag{1.13}$$

where $c$ denotes the speed of light, $\epsilon_{reff}$ represents the substrate's effective dielectric constant,$L_{eff}$ is the patch element's effective length, and $\Delta L$ shows the extension in patch length due to fringing fields.

### 1.3.2 Feeding Techniques

A very important factor in antenna performance is feeding technique. If the feed line is not carefully chosen, the antenna performance will be prone to degradation due to mismatching between the feeding and radiating element. Other constraints, including bending and junctions, lead to feed line discontinuities that result in surface loss and reduced radiation. The common feeding methods for exciting printed microstrip antennas are listed below.

- Coaxial feed
- Microstrip line feed
- Aperture coupled feed
- Proximity coupled feed

#### 1.3.2.1 Coaxial Feed

Commonly used techniques for feeding the microstrip antennas are coaxial probe feeding and the basic geometry of the coaxial feeding structure is shown in Fig.

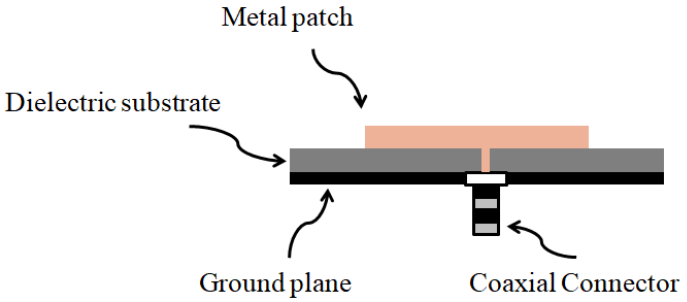


FIGURE 1.10: Geometry of coaxial fed patch antenna [9].

1.10. In this method, the shield and inner conductor of the coaxial connection are soldered to the ground plane and the radiating patch, respectively. Coaxial feeding has the characteristics of simple impedance matching and reduced spurious radiation as compared to microstrip line. This method increases antenna impedance by ensuring tight contact between the source and the load. One disadvantage of employing coaxial fed antennas is their low impedance bandwidth. If long probes are employed to increase bandwidth, they must be long enough to penetrate thick substrates deeply. Unwanted radiation from the probe will be a problem if the length is extended over the threshold limit as a result of an increase in surface current and a rise in feed inductance. Coaxial feed is only used with large, conventional antennas [9, 21]. Another drawback of the coaxial feeding method is a mismatch between simulation and fabrication performance. It is mostly caused by mismatch errors and incorrect injection of the inner probe during fabrication injection of the inner coax feed.

#### 1.3.2.2 Microstrip Line Feed

By employing this technique, the feed is given at the edge of the radiating element as shown in Fig. 1.11. A conducting strip that is thinner than the radiating patch is directly connected to the radiating patch. It is simple to fabricate since the microstrip feedline and radiating element are both on the same plane. To obtain the required impedance match, this method may use the inset technique. Due to its ability to carefully select the inset placement, no additional matching component

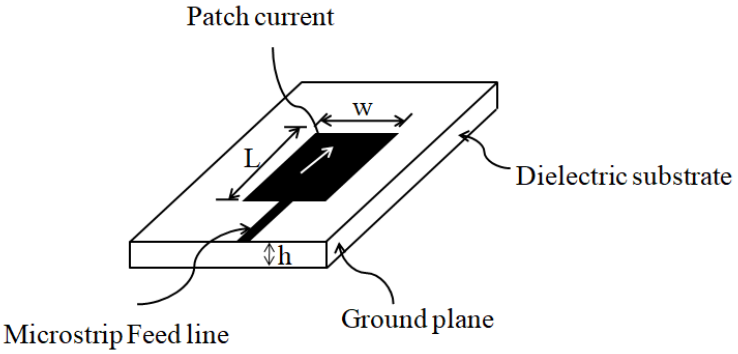


FIGURE 1.11: Geometry of microstrip line fed antenna [9].

is required. The use of this approach in planar antennas is fairly common due to its simplicity and ease of manufacture. The disadvantage of this feed is that when substrate thickness increases, spurious radiation and surface waves also tend to rise, which reduces antenna bandwidth. Furthermore, the feeding method has cross-polarization effects.

#### 1.3.2.3 Aperture Coupled Feed

The aperture coupled feed was introduced in 1985 [22]. Since then, it has gained popularity as a vital feeding method for microstrip patch antennas. The structure of the aperture coupled feed is illustrated in Fig. 1.12. In an aperture coupled microstrip patch antenna, the bottom of a dielectric substance known as the feed substrate comprises a microstrip feed line. A ground plane with an aperture/slot is situated on top of this substrate. Air or any material with a low permittivity may be present on top of the ground plane. This substance is followed by a layer of another dielectric substrate, and then on the top layer there is a radiating patch. The radiating element and feed line are not in the same plane, and the excitation current is fed to the radiating patch electromagnetically via an aperture or slot, resulting in an aperture coupled antenna. The isolation between the antenna and feed circuit, the elimination of probe reactance, and the flexibility of integrating arrays and active circuits are a few of the benefits of aperture coupled patch antenna. There is no direct connection between the radiating element and the feed

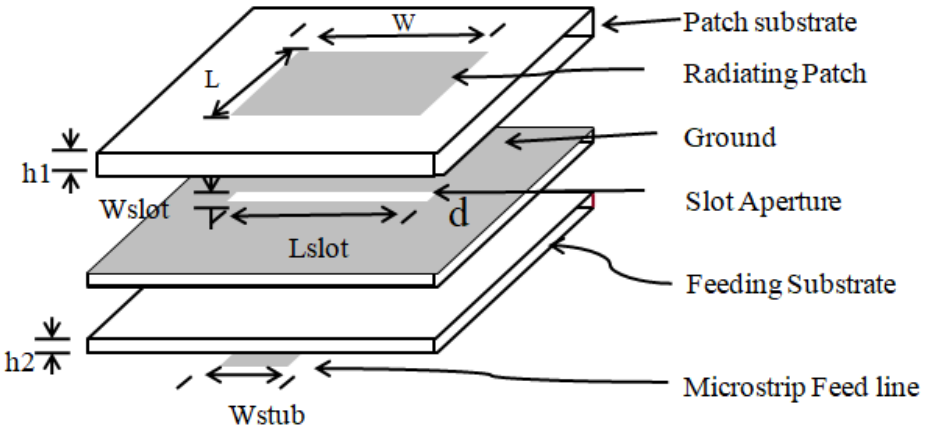


FIGURE 1.12: Geometry of aperture coupled patch antenna [22, 24].

line, so a wide micro strip line is avoided, which is critical for millimeter wave applications [22]. Radiation from the feed line to the patch is isolated by the ground layer between them [22]. Different techniques have been employed to enhance the inherent drawback of narrow bandwidth for microstrip patch antennas. Targonski and Pozar increased the impedance bandwidth of a stacked aperture-coupled feed by 50 to 70% in 1998 [23]. One of the drawbacks of this configuration is back-lobe radiation, but it can be mitigated by adding a second ground layer beneath the feeding network that acts as a reflector, as recommended by Pozar in 1996 [24].

#### 1.3.2.4 Proximity Coupled Feed

A proximity-coupled feed is also an electromagnetically coupled feed. Two dielectric substrates are required in this form of feed, with the feed line situated between the two substrates.

As shown in Fig. 1.13, the upper substrate is on top of the radiating patch, and the other substrate is below the feed layer. Compared to direct feeding systems, it has the advantage of having an incredibly high bandwidth performance. Individual performance can be improved in this approach since feed lines and patch lines have different substrates. The analysis of a structure with more layers is

more complicated, and the cost of manufacture is also high due to the more layers Moreover, fabrication is also a drawback of this design due to the alignment procedure [9, 25].

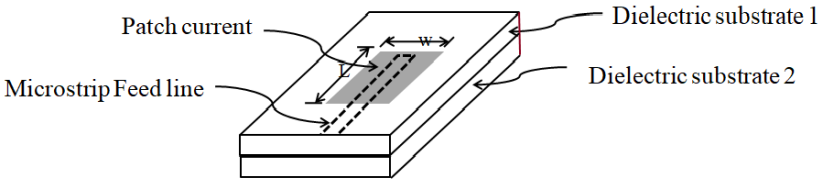


FIGURE 1.13: Geometry of proximity coupled patch antenna [9, 25].

## 1.4 Analysis Methods

The transmission line model, the cavity model, and the full wave model are the three that are most frequently used to study microstrip patch antennas [26]. The simplest of all is the transmission line model, but it is also the least effective. It gives useful physical understanding. Cavity models are more intricate, but they are also more precise and useful for understanding how physical processes operate.

### 1.4.1 Transmission Line Model

In transmission line model, two slots serve to represent the microstrip patch antenna, separated by a low-impedance transmission line of length $L$. When compared to other methods, the results we obtain are not the most accurate. It is adequate for creating the antenna. It is simple to manufacture the antenna model by using a transmission line.

### 1.4.2 Cavity Model

The area between the microstrip patch and the ground plane is, in accordance with research on microstrip antennas, a resonant cavity surrounded by magnetic

walls along the conductor's edge and the top and bottom of electric conductors. If the microstrip antenna is merely considered as a cavity simulation, the amplitude of the electric and magnetic fields cannot be estimated in the cavity model [26]. It gives a mathematical explanation for the magnetic and electric fields of a microstrip antenna. The antenna is modeled as a cavity filled with dielectric material to achieve this. Perfect electric conductors are used to symbolize the patch and ground plane, while magnetic barriers with sound electrical properties are used to symbolize the substrate's edges. It should be highlighted that the cavity model does not account for feed effects. The dielectric substrate is treated as a cavity, with top and bottom electric walls. Although the substrate must be quite thin, the patch seems normal.

## 1.5 Performance Analysis of Microstrip Patch Array

A low-profile single antenna has a gain of less than 10 dB [27]. Single antenna elements, such as a microstrip antenna, are capable of no more than about 10 dB gain. This cutting-edge arrangement of antenna formed by combining several microstrip antennas is known as a "microstrip antenna array". Fortunately, microstrip patch antennas are inherently compatible and can be integrated into array structures. An array can enhance the bandwidth while also providing higher levels of gain and directivity and enhancing various other functions as compared to a single microstrip antenna. The microstrip array antenna has the provision to construct the feed network and radiating elements on the same single-layer printed circuit board (PCB). As various microwave components, such as phase shifters, amplifiers, and switches, are manufactured as microwave MMIC on a single substrate, the microstrip antenna is advancing towards full integration, such as low frequency.

There are numerous variants of the microstrip array antenna. Microstrip Phase arrays are used in fixed phase applications due to fabrication simplicity. In order

to solve the grating lobes issue, the spacing between radiating elements should be smaller than $\lambda$ and higher than $\lambda/2$ to provide space for the feed network. More elements can be utilized to improve gain, but doing so will make the array larger in size. Just like every array, a microstrip array's shape can be linear, planar, or conformal, and its feed mechanism can be series or parallel. A planner array with a feed network that produces equal amplitude and phase [27]. In order to improve performance in terms of directivity and gain, the number of elements must be increased. This is one drawback of the array arrangement. Due to this, the structure's overall size increases, which is contrary to modern industrial requirements. For the optimal array performance, recent research has focused on several methods, such as using FSSs with an array [6].

### 1.5.1 Performance Parameters of Microstrip Patch Antenna

#### 1.5.1.1 Field Patterns

Field patterns associated to the antenna Radiating energy and reactive energy are two different types of energy that are related to them and varies with proximity. As a conclusion, there are three major areas that may be distinguished in the field around an antenna which are:

**1.5.1.1.1 Reactive near-field region** The area enclosing the antenna is termed as the reactive near-field. The reactive field is dominant in this area. In this location, energy is simply stored and is not wasted.

**1.5.1.1.2 Radiating near-field region (Fresnel region)** This area lies between the reactive near-field region and the far field region. Compared to the reactive near field region, radiation fields dominate here. Compared to the reactive near field region, radiation fields dominate here. The distribution of the angular field in this area depends on the distance from antenna.

**1.5.1.1.3 Far-field region (Fraunshofer region)** The zone beyond the near-field region is Fraunshofer region; there are no reactive fields; only the radiation fields exist here. The distance from the antenna has no effect on the angular field pattern. The power density in this region fluctuates as the inverse square of the radial distance, while the angular field pattern is irrespective of the antenna's distance.

### 1.5.1.2 Reflection Coefficient Γ and Characteristic Impedance ($Z_0$)

When evaluating implementations at higher frequencies, it is important to take into account the idea of reflection that takes place in microwave transmission lines. Each transmission line has intrinsic impedance, which originates from the way the line is constructed and consists of resistance and reactance. This impedance is known as its characteristic impedance, ($Z_0$). However, a reflected wave will be developed if the transmission line is terminated with a load that is not equal to its characteristic impedance ($Z_L \neq Z_0$), this phenomenon is known as reflection coefficient, Γ.

$$\Gamma = \frac{Z_L - Z_0}{Z_L + Z_0} \tag{1.14}$$

### 1.5.1.3 Return Loss ($R_L$)

The amount of power that an antenna reflects back rather than radiates is measured by a metric called return loss. When the transmitter and antenna have unequal impedances, standing waves are formed.

$$R_L = \log|\Gamma|(dB) \tag{1.15}$$

### 1.5.1.4 Directivity and Gain

As compared to the radiation intensity in a given direction to that of an isotropic antenna, an antenna's directivity measures how much of the energy it radiates is concentrated in the main beam direction. Whereas calculating the gain G, antenna

related losses are taken into account so it is slightly less than the directivity (D). The antenna-related losses are taken into account in calculating the gain G, that is a little less than directivity. Directivity D and gain G are connected by radiation efficiency ($e_r$).

$$G = e_r \times D \tag{1.16}$$

where G, $e_r$ and D are Gain, radiation efficiency and directivity respectively.

Conduction, dielectric, and surface wave inefficiencies connected to the structure are taken into account by the radiation efficiency ($e_r$), which is computed as the ratio of the output power to the input power.

#### 1.5.1.5 Impedance Bandwidth

The impedance bandwidth of the antenna is the band of frequencies outside this span impedance magnitude is less than the half of the resonant magnitude. Within this band of frequencies, the antenna might be efficiently utilized. VSWR will cause significant reflection of input Power due mismatch of impedance.

## 1.6 Frequency Selective Surface

In the 18th century, American scientist David Rittenhouse found that when a city lamp is examined through a silk handkerchief, some colors of the light spectrum are suppressed. The handkerchief's ability to be frequency selective, demonstrated that surfaces may display various transmission characteristics depending on the frequency of the incoming wave. Hence, these surfaces are now called FSSs [28]. An FSS may be thought of as a free-space filter that can be used to pass some frequencies while blocking others. By creating periodic geometric metallic patterns on a dielectric, these spatial filters are created, as shown in Fig. 1.14. Imagine an incident wave striking a metal surface to better comprehend the idea of spatial filtering, as shown in Fig. 1.15. A single electron with a direction vector perpendicular to the plane is shown as being in the surface plane. The incident wave's

E-vector is parallel to the metallic surface. The electron is therefore forced to accelerate in the direction of the E-vector when the incident wave impacts the metal surface. Therefore, a portion of the energy must be transformed into the kinetic energy of the electron in order to maintain the electron's constant oscillation. As a result, the electron will absorb the majority of the incoming energy and reflect it. If all of the incident wave's energy is transferred to the kinetic energy of the electron, there will be no transmission through the filter.

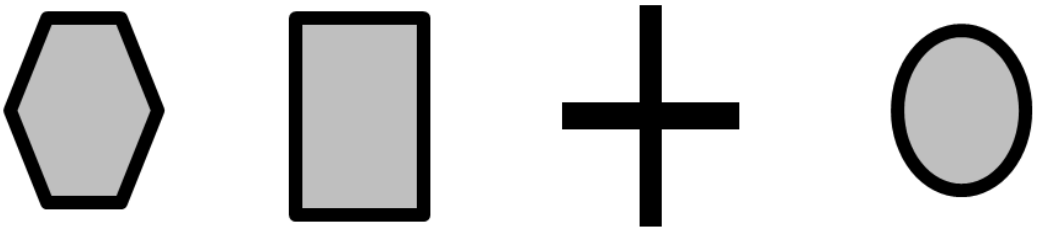

FIGURE 1.14: Several prominent element shapes used in FSS designs [28].

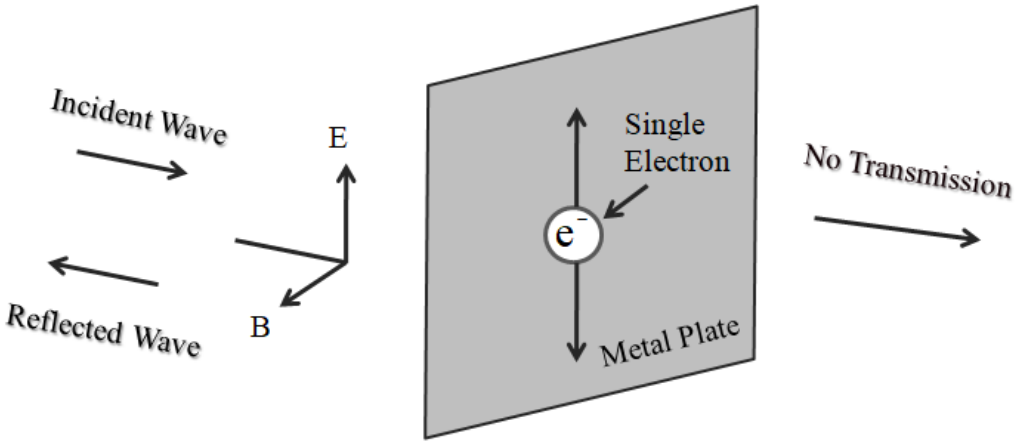


FIGURE 1.15: Low transmittance results from the oscillation of the electron in the plane caused by the force of the incident wave [28].

Using the example of Fig. 1.16, where the direction vector of the electron is perpendicular to the incoming wave's E-vector. In this instance, the electron is compelled to proceed down the direction vector despite the force of the E-vector.

As a result, the electron is unable to absorb the incident wave's kinetic energy. There is a high transmittance as a result of the wave not being absorbed.

To carry out a filter operation, FSSs may be singly, twice, or three times periodic. It is also typical to stack many FSSs, often with a dielectric layer between each one. According to their physical nature, composition, and geometry, FSSs may be classified into four different filter types, which are detailed in subsection 1.6.1. A triply periodic FSS utilizing cross dipoles is depicted in Fig. 1.17 and is comparable to a three-dimensional (3D) photonic crystal.

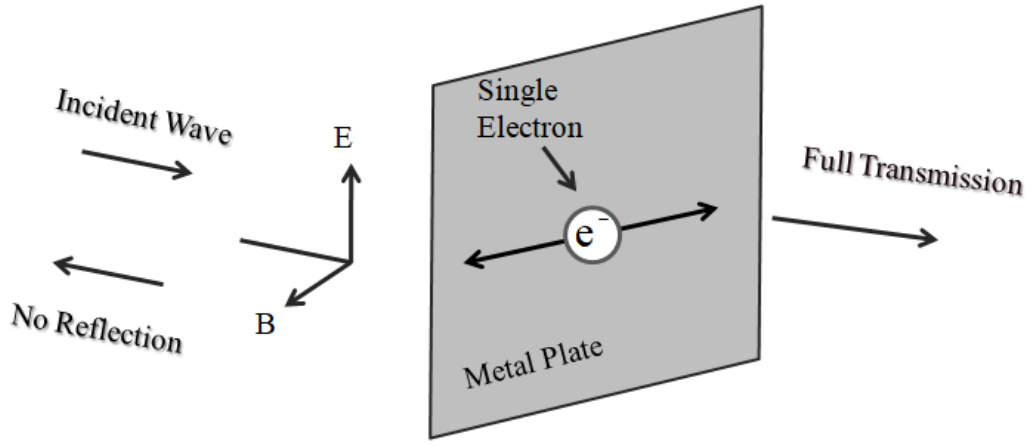


FIGURE 1.16: Electron is constrained to move and hence unable to absorb energy resulting in high transmittance [28].

### 1.6.1 FSS Types

FSSs are filters that may be made to provide the four common filter responses of bandstop, bandpass, high-pass, and low-pass. If the structure is symmetrical, Babinet's approach may be used to transform the resposne from bandstop to bandpass, from low-pass to high-pass, and vice versa. This implies that the order of the conducting and non-conductive parts must be changed to convert a high-pass filter into a low-pass filter, as shown in Fig. 1.18. Depending on the design specifications, including the degree of attenuation, bandstop/bandpass frequency,

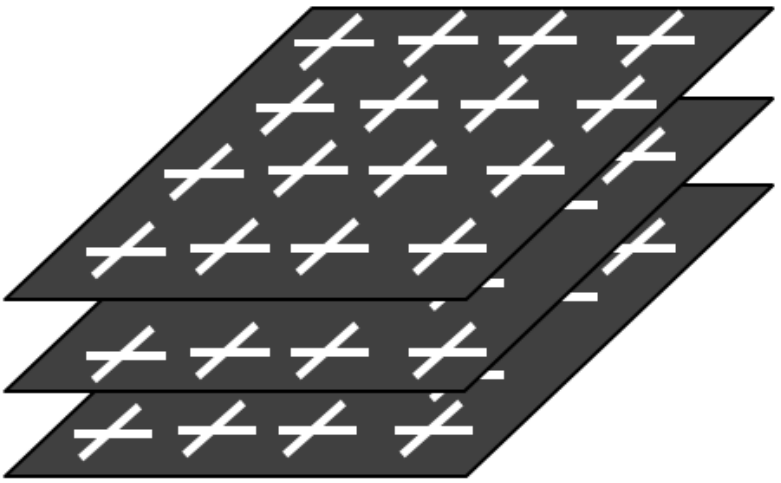

FIGURE 1.17: A cascaded FSS [28].

bandwidth, and sensitivity to electromagnetic wave incidence angle, a suitable FSS element is selected.

#### 1.6.1.1 Low-pass FSS

Typically, they are of the mesh type seen in Fig. 1.18(a). A conductive sheet may be perforated to create them (leaving behind an array of patches).

#### 1.6.1.2 High-pass FSS

According to Fig. 1.18(b), the high-pass FSS can be the low-pass FSS's Babinet complement, as shown in Fig. 1.18(a).

#### 1.6.1.3 Bandstop FSS

It manifests as periodic arrays of conductive components with the following geometries: cross dipoles, tripoles, square or hexagonal loops, etc. Most people have probably used this FSS. In Fig. 1.19(a), a typical cross dipole configuration is depicted.

#### 1.6.1.4 Bandpass FSS

Figure 1.19(b) depicts a conventional bandpass FSS. It is bandstop filter's Babinet complement which is shown in Fig. 1.19(a).

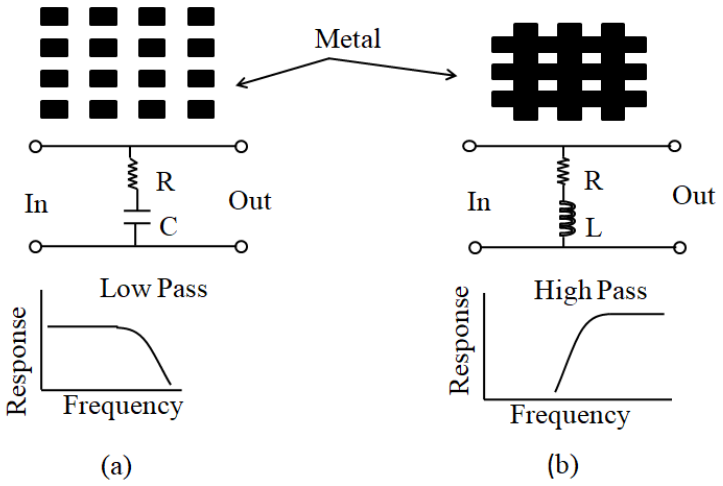


FIGURE 1.18: (a) Low-pass and (b) high-pass FSS along with their equivalent circuit models and transfer function [28].

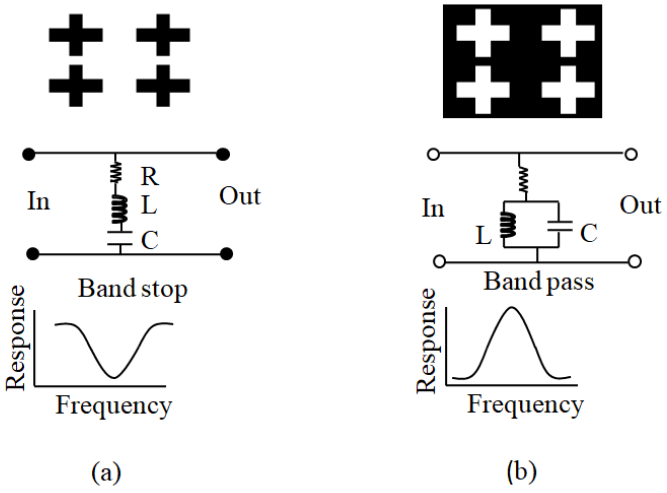


FIGURE 1.19: (a) Bandstop and (b) bandpass FSS along with their equivalent circuit models and transfer function [28].

### 1.6.2 Classification of FSS

Depending on the capacity to dynamically adjust the spatial filtering properties, an FSS may be divided into two categories. The two main types are:

1. Passive FSS
2. Active FSS

A passive FSS is one that fabricates periodic structures on a dielectric sheet to transmit or reflect a specific frequency. Once created, the characteristics of this surface cannot be changed.

The key requirement in this case is that they must be large enough to be pasted on a significant portion of a wall or window in order to either pass or block the required signal. These FSSs have the benefit of being simple to build and design, but they also have the drawback of being non-configurable. Figure 1.20 depicts a 3×3 array of passive cross-dipole FSS.

In contrast, an active FSS is composed of periodic structures that include active components like PIN diodes or varactor diodes (see Figure 1.21). The FSS can be modified by adjusting these active devices in response to an external stimulus (DC power source). The expense of production, energy consumption, and the requirement for a DC power supply are some of the drawbacks of such surfaces.

### 1.6.3 Analyzing an FSS

The phased array antenna theory provides the theoretical framework for FSSs. The methods for analyzing FSS filters are several and are discussed in this section.

#### 1.6.3.1 Circuit Theory Technique

This method derives the equivalent circuit model for the FSS using a quasi-static approximation. It only offers findings that are quite accurate for straightforward FSS designs with typical incidence. However, simulating an analogous FSS circuit with oblique incidence is challenging and may not produce results that are very precise (as compared to full wave simulations).

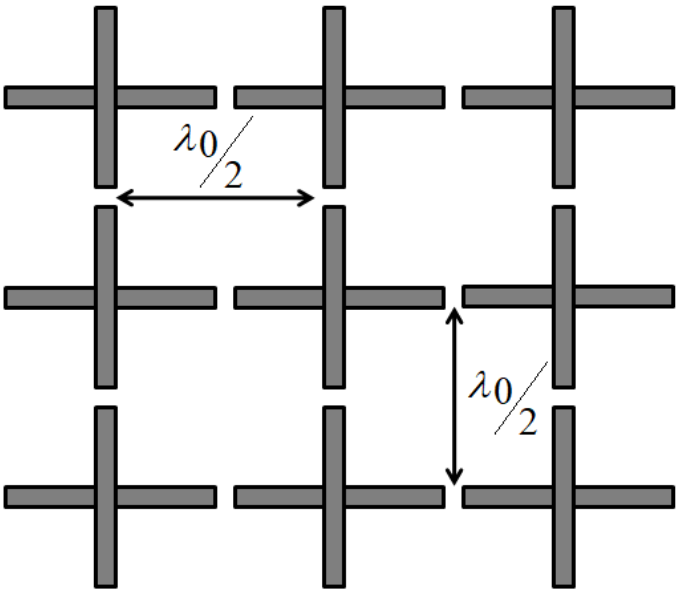


FIGURE 1.20: A finite 3×3 passive cross-dipole FSS.

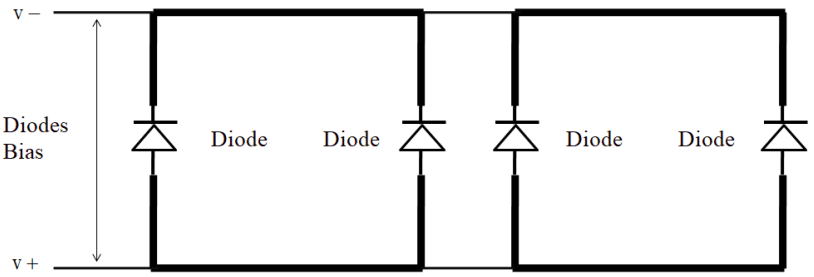


FIGURE 1.21: An active square loop FSS with PIN diodes.

#### 1.6.3.2 Model Expansion Technique

The aperture modes and Floquet modes in space are matched in the model expansion procedure to create an integral equation. The method of moments or the conjugate gradient method are then used to solve this integral problem.

#### 1.6.3.3 Iterative Technique

This method uses iteration to get around the need for a lot of matrix storage. Iterative current flow occurs on the conducting region's surface. The spectral

response of FSSs may be predicted with good accuracy using this technique as well.

### 1.6.4 Applications of FSS

A FSS could be employed in a variety of engineering applications, including:

- RFID tags
- Collision avoidance
- Radar cross-section (RCS) augmentation
- Gain enhancement of antenna
- Electromagnetic interference (EMI) protection
- Subreflectors in parabolic reflector antennas
- Radomes
- Waveguide or cavity control coupling
- Communication system security

## 1.7 Research Problem

In recent years, the need to design high-gain antennas has shown a sharp and rapid increase. To achieve this goal, antenna elements are arranged in an array configuration. Although the array provides high gain and narrow beamwidth, it does so at the expense of its large size. One way to enhance the gain is to integrate a FSS reflector above or below the antenna array. Furthermore, FSS reflectors have physical capabilities that can be used to focus the radiated field for the sake of antenna gain enhancement.

## 1.8 Research Objective

The objective of this research is to develop an FSS integrated high gain aperture coupled patch antenna array for X-band applications. In addition, it is established that the designed array should provide low SLLs and narrower beamwidth in the band of interest.

## 1.9 Thesis Outline

The research thesis is organized in the following way:

**Chapter 1** starts with the background of antennas and their origins. After that, the antenna arrays and their types are discussed in detail. In addition, the design of a basic microstrip patch antenna is discussed along with its feeding techniques and analysis methods. The chapter also provides a discussion on FSS. At the end of this chapter, a research problem and the objective of this research are presented.

**Chapter 2** discussed the designs of previously presented FSS-based antennas and antenna arrays.

**Chapter 3** provides a detailed discussion of the proposed aperture coupled patch antenna array. The chapter starts with the design of a single-element aperture coupled patch antenna. After that, the design of the aperture coupled patch antenna array is discussed along with the simulation results. For gain enhancement, an FSS is designed and integrated with the proposed array.

**Chapter 4** provides the conclusion.

# Chapter 2

# Literature Review

Microstrip antennas have attracted considerable attention since the 1970s [9]. Moreover, due the huge demand for high-gain antennas especially for satellite and radar applications, there is a need to design antenna arrays for these applications with compact size. Microstrip antennas are one of the examples of small size antennas. They consists of a very thin patch placed a small fraction of a wavelength above a ground plane. The array arrangement of microstrip antennas are also useful for radar and satellite applications, but they suffer due to their low gain. In the literature, many researchers utilized FSS reflectors to enahnce the gain of patch antennas. A detailed description about previously presented designs is given in the next section.

## 2.1 Related Work

In [29], the authors improved the performance of a U-slot patch antenna by using a dual-band FSS. The FSS design was composed of a modified Jerusalem cross-shaped element (see Fig. 2.1) to achieve resonance at 2.45 GHz and 5.8 GHz. It was observed from the results that the use of FSS superstrate offered peak gains of 4.69 and 6.54 dBi at 2.45 and 5.8 GHz, respectively. It was also noted that at 2.45 GHz, the gain was improved a little bit, but a significant improvement

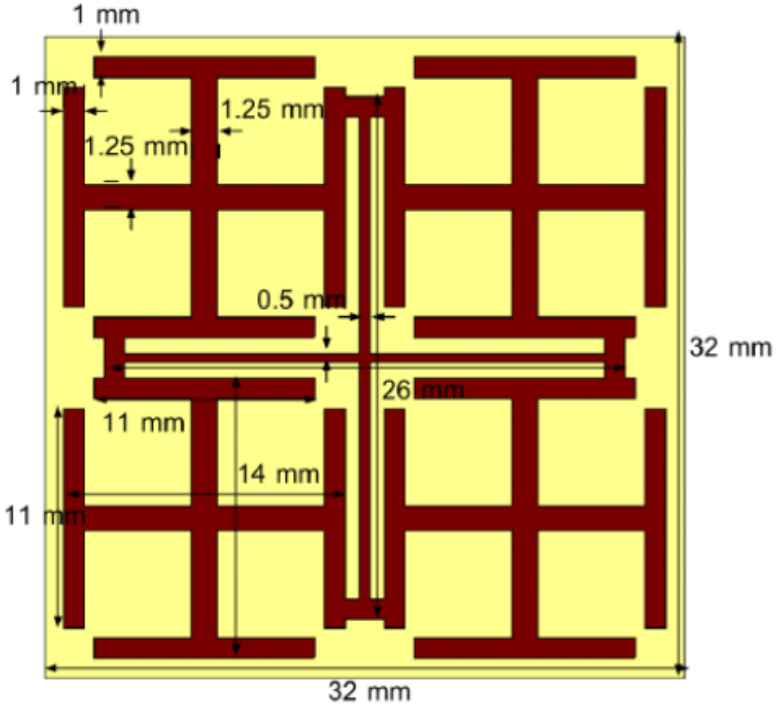


FIGURE 2.1: Design of the modified Jerusalem cross-shaped element [29].

in gain was observed at 5.8 GHz. In [30], the gain of the dual-polarized cavity reflex antenna was enhanced by using two types of FSS reflectors. One design consisted of a slotted cicular-shaped FSS, while the second design was composed of a slotted square-shaped FSS. It was observed that the gain of the antenna was increased in the range of 16-20 dBi for two orthogonal linear polarizations by using both the configurations. The same kind of configuration was used in [31]. In [32], a multiple square-loop elements-based FSS design was presented for bandwidth and gain enhancement of a dual-band patch antenna. The patch antenna was composed of a multilayer structure. The FSS superstrate was placed above the patch antenna to achieve high-gain for WLAN and WiMAX applications.

In [33], a wideband and high-gain mushroom-like antenna was designed with low RCS, as shown in Fig. 2.2. A modified square-loop FSS bandstop filter was designed so that it could reduce out-of-band frequency RCS without disturbing the gain. From the presented configuration, the authors achieved a wideband RCS reduction both in and out of the antenna operating frequency band and also enhanced the gain in the band of interest. In [34], a novel dual-band resonant cavity antenna with high gain and single polarization was presented. The gain of

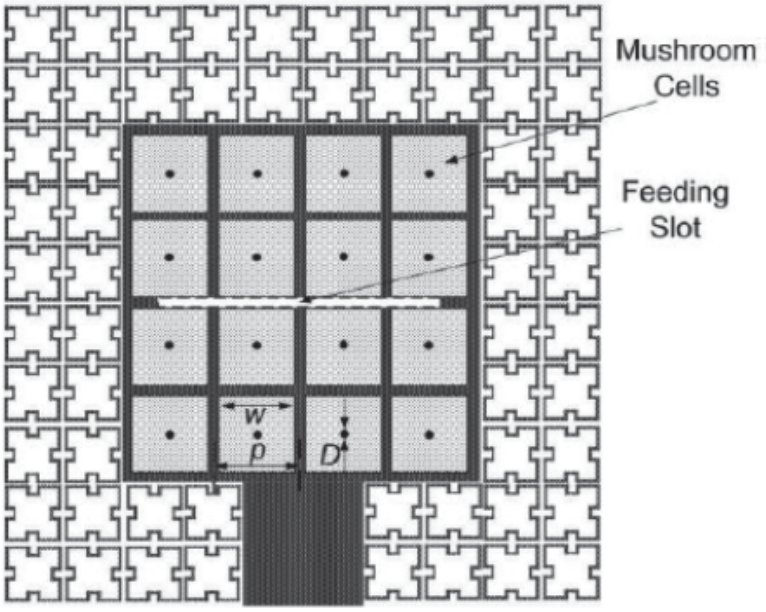


FIGURE 2.2: Geometry of the mushroom-like patch antenna with FSS bandstop filter [33].

the antenna was enhanced by using an array of conventional square patch FSS. The authors also designed a feeding system for dual-band operation. Two T-shape slots were introduced in the non-radiating edges of the patch, which serves as the feed system of the designed dual-band high-gain antenna. In [35], a novel FSS reflector was designed for the gain enhancement of patch antennas. Utilizing the single-layer and double-layer FSS reflector tends to a gain of 5.06 dBi and 6.86 dBi at 24 GHz. The authors of [36] also created a novel FSS reflector with high X-band gain. They observed that the use of an FSS reflector above the patch antenna tends to achieve a gain of 14.43 dBi.

In [37], a high-gain aperture coupled patch antenna design was presented for WLAN applications. For gain enhancement in the band of interest, a novel capacitive FSS was designed and its array was placed above the patch antenna. The results demonstrate that the presented configuration offered a peak gain of 6.67 dBi at 2.6 GHz. In [38], a high-gain circularly polarized stacked patch antenna was designed. To create dual-band properties, two patches are stacked one over the other on a single substrate. For high-gain, an FSS reflector operating at 2.4 GHz or 3.5 GHz was used. For the proposed configuration, a gain of about 8.9 dBi and 3.9 dBi was achieved at 2.2 GHz and 3.6 GHz. It was also observed that

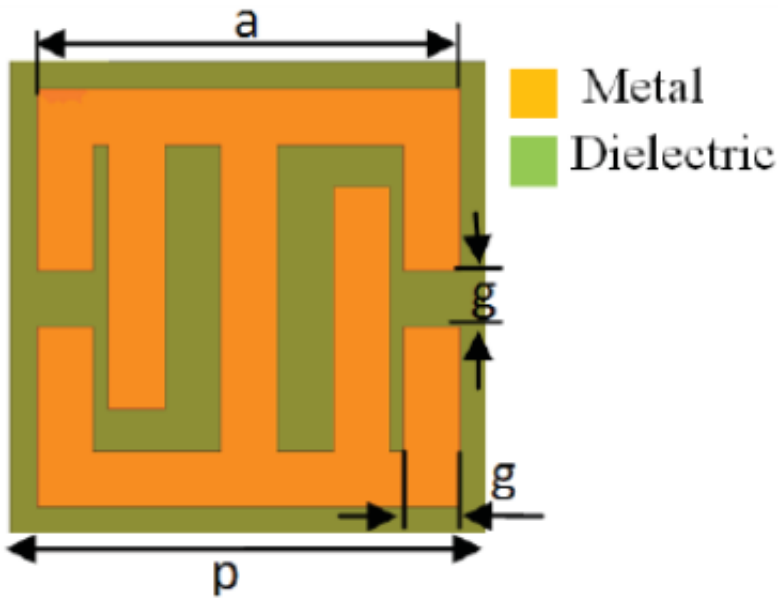


FIGURE 2.3: Design of the novel FSS unit-cell operating at 28 GHz [41].

the use of FSS does not affect the axial ratio (AR) of the antenna. In [39], a wideband FSS superstrate was designed for gain enhancement of an antenna at millimter-wave (mmwave) frequencies. This FSS structure was composed of two metals separated by a dielectric substrate. The designed FSS was placed above the two-layered patch antenna to achieve a maximum gain of 12.9 dBi in the 60 GHz frequency band. In [40], a multilayer patch antenna was designed for mmwave 24 GHz applications. A substrate-integrated suspended line (SISL) technology was utilized for the design of the patch antenna. The patch antenna was embedded between the dielectric layers while the FSS layer was placed on top of the dielectric substrate. It was observed that the SISL technology with FSS superstrate offered a wideband response and 10 dBi gain at 24 GHz. In [41], the authors presented a novel FSS design (see Fig. 2.3) for the gain of enhancement of microstrip patch antenna in the 28 GHz frequency band. It was observed that the FSS-based patch antenna achieved a high-gain of 6 dBi for the frequency band of interest.

In [42], an FSS-loaded high gain patch antenna array was designed for WiMAX, WiFi, and WLAN applications. A 1×2 linear array was designed. The structure of the single antenna was composed of a Z-shaped radiating element. Each antenna element was fed through a novel 1×2 corporate feeding network. Furthermore, the FSS unit-cell design consists of a simple modified slotted square patch element.

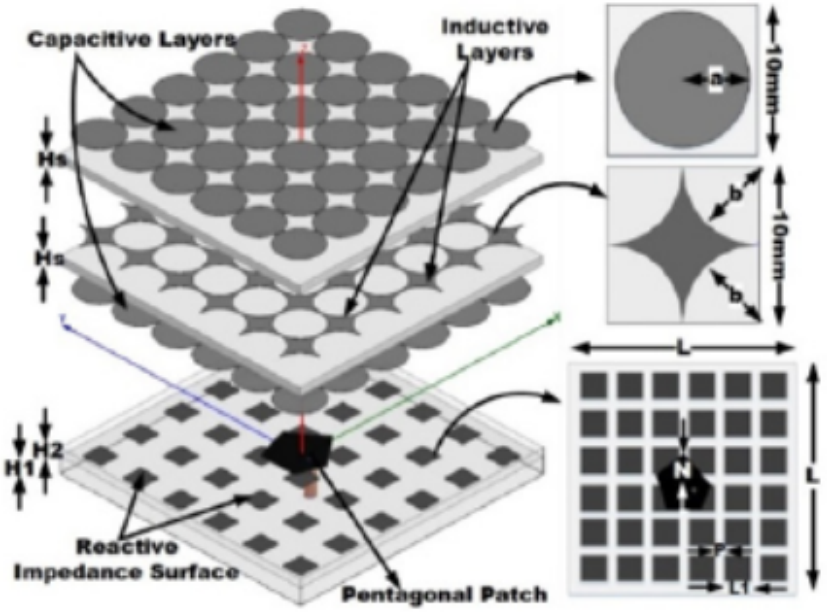


FIGURE 2.4: 3D view of pentagonal patch antenna loaded with highly reflective surface and reactive impedance surface [45].

The authors achieved a gain of 11.8 dBi at 5.8 GHz with the use of an FSS reflector. In [43, 44], a dense dielectric (DD) aperture coupled patch antenna was designed for mm-wave applications. For gain enhancement, the authors designed a modified circular FSS-based highly reflective superstrate and placed it above the patch antenna, and observed a peak gain of 17.78 dBi at 28 GHz. They also designed a partially reflective surface (PRS) for the band of interest, and achieved a gain of 15.4 dBi.

In [45], the authors used highly reflective surfaces and reactive impedance surfaces to enhance the gain of the pentagonal patch antenna. The reflective surface was composed of two capacitive layers and one inductive layer, which was embedded between the capacitive layers, as shown in Fig. 2.4. In the design, the reactive impedance surface was placed between the patch and the ground plane, while the FSS layer was placed above the patch antenna. This type of configuration tends to achieve a gain of approximately 12 dBi in the band of interest with circular polarization.

In [47], the authors designed a bandpass slotted square-shaped based FSS supestrate to increase the gain of a wideband modified square planar monopole antenna.

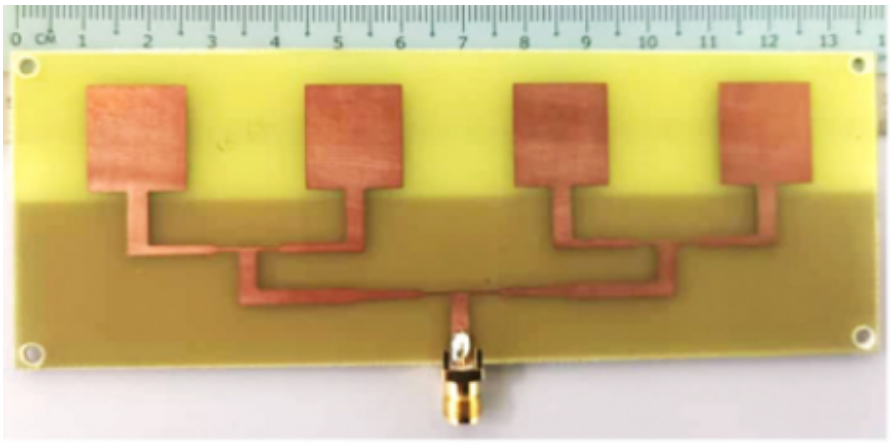

(a)

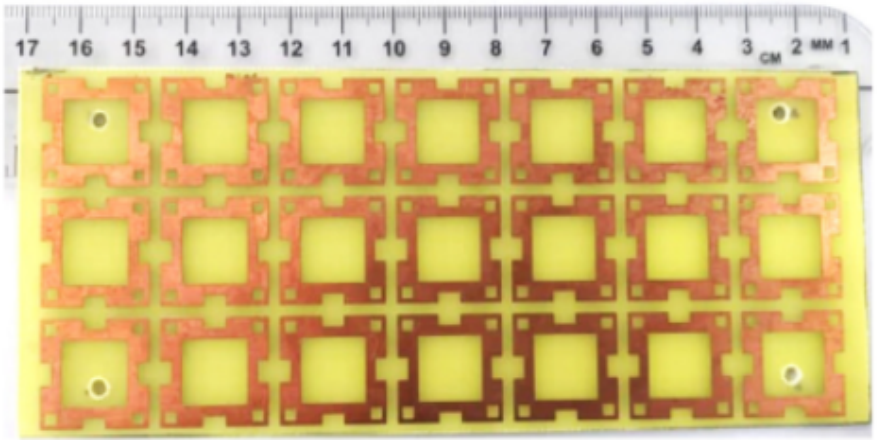

(b)

FIGURE 2.5: (a) Design of a 1×4 conventional rectangular patch antenna array [46] (b) Design of the modified square-loop FSS superstrate [46].

A gain improvement of about 6.5 dB was observed in the operating bandwidth by placing the FSS superstrate behind the antenna. In [48], a wideband and high-gain printed antenna was designed for sub-6 GHz fifth-generation (5G) applications. The antenna design was composed of a conventional rectangular patch backed by a partial ground plane. The wideband response was achieved by incorporating a circular slot into the ground plane. To achieve high-gain, a conventional dual square-loop FSS reflector was designed. It was observed that the proposed antenna with FSS offers a peak gain of 5.5 dBi in the frequency band of interest.

In [49], the authors enhanced the gain of an ultra wideband (UWB) planar monopole antenna with the help of a conventional ring-shaped FSS superstrate. They achieved an average gain of 5.9 dBi and a peak gain of 9.2 dBi in the UWB

range. A design of an FSS integrated 1×4 linear array antenna for sub-6 GHz applications was presented in [46]. The four-element array was composed of a conventional rectangular patch of elements fed through a corporate feeding network, as shown in Fig. 2.5(a). The wideband response was achieved with the use of partial ground plane (see Fig. 2.5a). To enhance the gain, a novel modified square-loop FSS superstrate, shown in Fig. 2.5(b) was placed behind the array and achieved a peak gain of 12.4 dBi in the frequency band of 3.5-5.8 GHz.

In [50], the authors increased the gain of a UWB diversity slot antenna by using a novel shaped FSS superstrate. As shown in Fig. 2.6(a), the antenna elements are semi-arc-shaped radiating elements, while the ground plane is an open-ended ring radiator. For FSS superstrate design, a square-ring element with a diamond-ring strip inside it was used (see Fig. 2.6b). From the presented configuration, they achieved a gain of >8 dBi in the UWB frequency band. In [51], the authors enhanced the gain of a mmwave slot antenna by using an FSS cell, which was composed of two metallic rings connected to a rectangular strip. From the results, the authors observed a 5.3 dB increase in gain in the band of interest. The peak gain noted in the operating bandwidth is equal to 10.3 dBi.

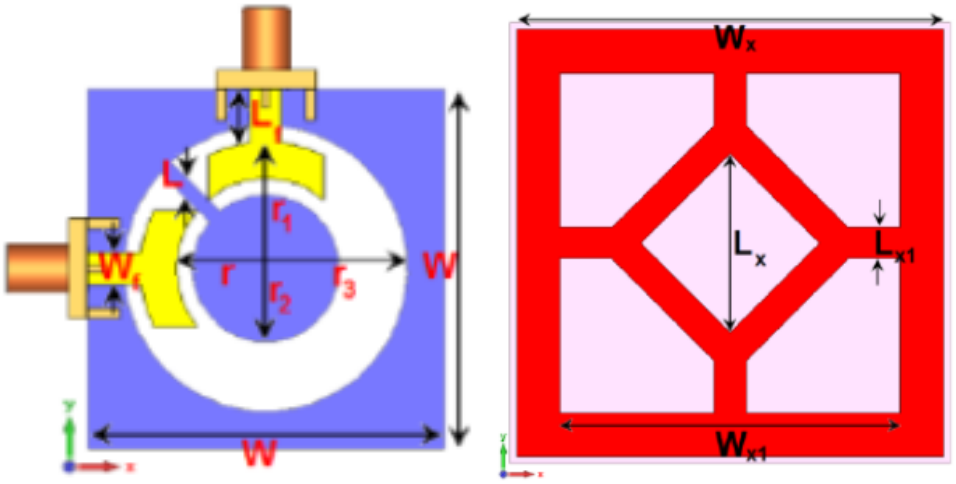


(a) (b)

FIGURE 2.6: (a) Design of a UWB diversity slot antenna [50] (b) Design of the novel FSS superstrate [50].

The performance comparison of the above-presented FSS-based antennas is presented in Table 2.1. The comparison is done in terms of antenna type, FSS type,

frequency bands, and peak gain.

TABLE 2.1: Performance comparison of previously published FSS-based antennas.

| Ref. | Antenna Type | FSS Type | Frequency Band (GHz) | Peak Gain (dBi) |
|---|---|---|---|---|
| [29] | U-slot patch | Modified Jerusalem cross | 2.45/5.8 | 4.69/6.54 |
| [30, 31] | Cavity reflex antenna | Slotted square | 10 | 20.87 |
| | | Slotted circular | 10 | 20 |
| [32] | U-slot patch | Multiple square-loops | 2.45/3.5 | 9.3/7.3 |
| [33] | Mushroom-type | Modified square-loop | 4.5-5.8 | 10 |
| [34] | Resonant cavity antenna | Square patch | 6.95/13 | 16.5/20.9 |
| [35] | Rectangular patch | Single layer FSS | 24 | 5.06 |
| | | Double layer FSS | | 6.86 |
| [36] | Rectangular patch | Y-shaped ring | 9.5 | 14.43 |
| [37] | Aperture coupled patch | Capacitive FSS | 2.6 | 6.67 |
| [38] | Stacked patch | Metallic strips | 2.2/3.6 | 8.7/3.9 |
| [39] | Multilayer patch | Dual-sided FSS | 60 | 12.9 |
| [40] | SISL-based patch | Rectangular patch | 24 | 10 |
| [41] | Rectangular patch | Modified square | 28 | 6 |
| [42] | 1×2 patch array | Modified slotted square | 5.8 | 11.8 |
| [43, 44] | DD patch | Highly reflective | 28 | 17.78 |
| [45] | Pentagonal patch | Highly reflective | 5.3 | 12 |
| | | Reactive impedance surface | | |
| [47] | Modified square monopole | Slotted square patch | 2.45 | 7.5 |
| [48] | Rectangular monopole | Dual square-loop | 3.32-4.2 | 5.5 |
| [49] | UWB planar antenna | Ring | 1.9-15.2 | 9.2 |
| [46] | 1×4 patch array | Modified square-loop | 3.5-5.8 | 12.4 |
| [50] | Diversity slot antenna | UWB FSS | 3.1-10.6 | >8 |
| [51] | Slot antenna | Metallic rings | 25.2-31 | 10.3 |

## 2.2 Problem Statement

From the above-presented literature and from Table 2.1, it is observed that most of the researchers are focused on the gain enhancement of single antenna elements. Very limited information is available for the gain of antenna arrays using FSS or

highly reflective surfaces. In addition, some of the researchers utilized multilayer strucutres, which offers additional complexity in the design. Furthermore, most of the researchers designed antennas for commercial applications. So, there is a need to design a high-gain antenna array for radar and satellite applications. Moreover, it is necessary to design a simple FSS-based antenna or antenna array that can easily be fabricated and integrated into the system.

## 2.3 Thesis Contribution

In this thesis, the design of a 1×4 linear aperture coupled patch antenna array is designed and presented for X-band satellite communication applications. For the design of the array, a conventional aperture coupled patch element is selected. To enhance the gain of the proposed array, a novel modified square-loop FSS reflector operates in the 10 GHz frequency band. The FSS superstrate is placed on the back side of the antenna array at a specific distance. From the presented results, it is observed that the proposed array offers a wideband response in the frequency band of interest. The noted impedance bandwidth is equal to 1.09 GHz, ranging from 9.39 to 10.48 GHz. Furthermore, a peak gain of 11.2 dBi is achieved with SLLs of 16.7 dB at a center frequency of 10 GHz.

## 2.4 Summary

This chapter presents the designs of previously published FSS-based antennas for different communication applications. From the presented literature, it is established that very few FSS-based array designs are presented in the literature, and none of them designed FSS-based arrays for satellite applications. In the last part of this chapter, a thesis contibution is presented, which shows what will be presented in this work.

# Chapter 3

# FSS-based Aperture Coupled Patch Array Antenna for X-band Applications

In this chapter, the design of an FSS-based aperture coupled patch array antenna for X-band applications is presented. A complete design procedure is described along with the results. The proposed array is designed in three steps. First of all, the design of the single aperture coupled patch is optimized to achieve resonance for the 10 GHz frequency band. In the second step, a four-element linear array is designed to achieve high-gain at the desired frequency band. To further enhance the gain and to achieve low SLLs, an FSS reflector is designed with the proposed array. The FSS reflector is designed to operate in the 10 GHz frequency band.

## 3.1 Design of Aperture Coupled Patch Antenna

The design of the conventional aperture coupled patch antenna is shown in Fig. 3.1. The antenna is designed according to the process presented in [9]. By using two dielectric substrates separated by a ground plane, an aperture coupled antenna avoids the direct electrical connection between the feed line and the radiating

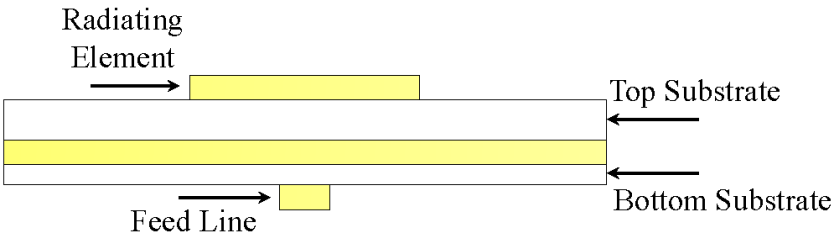


(a)

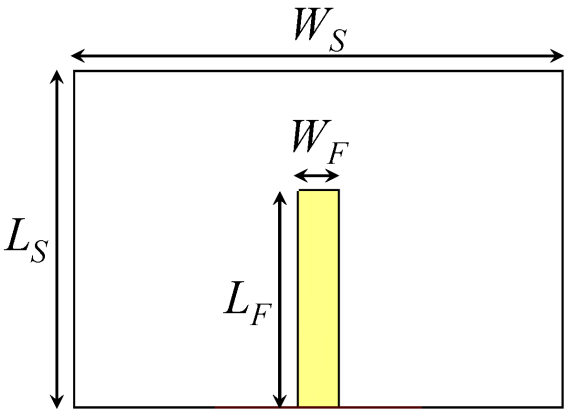


(b)

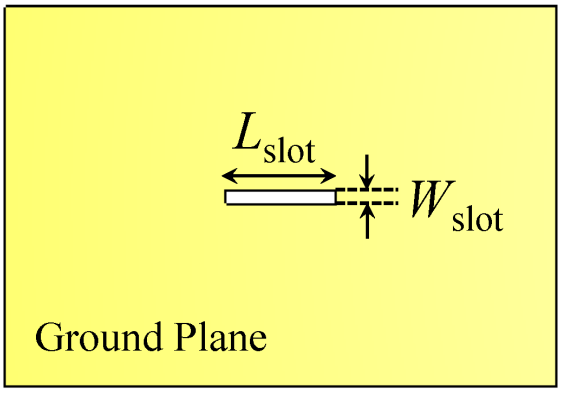


(c)

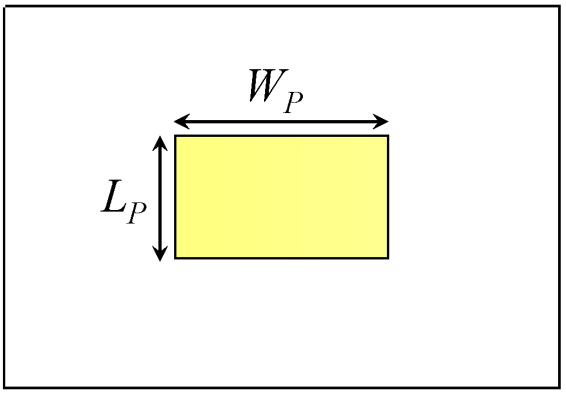


(d)

FIGURE 3.1: Design of the proposed aperture coupled patch antenna (a) side-view (b) bottom view with microstrip feeding line (c) ground plane with rectangular slot (d) radiating element on the top surface.

element. This makes it possible to independently optimize the radiating element and the microstrip feeding line. From Fig. 3.1(a), one can observe that the same kind of configuration is used to design the proposed antenna. The bottom layer's back side is made up of a 50Ω microstrip feeding line (see Fig. 3.1b), while the front side is made up of a ground plane with a rectangular slot (see Fig. 3.1c). The rectangular patch is printed on the top-side of the top (second) layer, as depicted in Fig. 3.1(d). The proposed antenna is designed on a low-cost FR-4 substrate having a relative permittivity of 4.4. The thickness of the bottom dielectric layer is taken to be 0.8 mm, while the top dielectric has a thickness of 1.6 mm. One can note that the top dielectric is thicker than the bottom dielectric, which is utilized to achieve a wide impedance bandwidth for the band of interest. The rest of the design parameters are listed in Table 3.1.

TABLE 3.1: Design parameters of the proposed aperture coupled patch antenna (all dimensions in mm).

| $W_S$ | $L_S$ | $W_F$ | $L_F$ | $W_{\text{slot}}$ | $L_{\text{slot}}$ | $W_P$ | $L_P$ |
|---|---|---|---|---|---|---|---|
| 24 | 16.5 | 2 | 10.6 | 0.6 | 4.75 | 9.25 | 5.25 |

### 3.1.1 Working Principle

In this sub-section, the operational mechanism of the aperture coupled patch antenna is discussed.

Two different operating modes are available for an aperture coupled patch. With relatively small apertures and thin substrates, tight coupling is simple to accomplish. The input impedance characteristic in this instance is that of the resonant patch as perceived via a step-down transformer. A small influence on resonant frequency is produced by increasing the aperture, which lowers the effective transformer ratio and raises input impedance. On the other hand, in thicker substrates, tight coupling is not obtained until the slot approaches the resonant length. The input impedance in this instance has the characteristics of two under-coupled resonators: a low-Q resonance caused by the patch at a lower frequency and a

high-Q resonance caused by the slot resonance at a higher frequency. It is possible to get acceptable impedance behavior across a large bandwidth by tuning these resonances [9].

Additionally, the patch above the ground plane can be thought of as a radiating cavity with resonant cavities at each end [9]. The half-wave patch's effective length is extended by the fringing fields, which causes it to typically be shorter than a half wavelength in the dielectric medium. The aperture couples energy into the patch cavity by interrupting the passage of current on the ground plane underneath the microstrip feed-line.

### 3.1.2 Simulation Results

The simulated reflection coefficient ($S_{11}$) of the proposed aperture coupled patch is shown in Fig. 3.2. It is observed that the designed antenna is able to resonate for the 10 GHz frequency band. The impedance bandwidth of the antenna, according to -10 dB bandwidth criteria, is noted to be 1.08 GHz ranging from 9.52 to 10.6 GHz, as shown in Fig. 3.2.

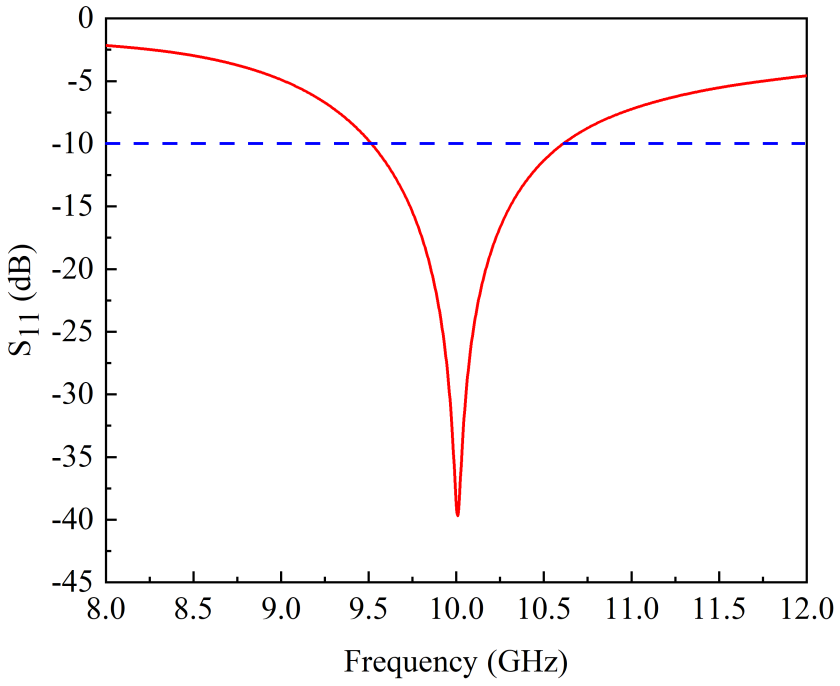


FIGURE 3.2: Simulated $S_{11}$ of aperture coupled patch antenna.

The radiation and total efficiency of the proposed antenna is shown in Fig. 3.3(a). The radiation efficiency of the antenna fluctuates in the range of 66.24-70.6% in the band of interest, while the total efficiency varies from 60% to 70.5%, as shown in Fig. 3.3(a). The realized gain of the antenna varies in the range of 4.35-5.06 dBi in the operating bandwidth (see Fig. 3.3b). From the presented results, it can be said that the designed antenna is able to provide acceptable radiation efficiency and gain for the band of interest.

The normalized H-plane radiation characteristics of aperture coupled patch antenna are shown in Fig. 3.4. It is observed that the main beam is directed towards 0° (see Fig. 3.4), which shows that the antenna exhibits directional radiation characteristics. Furthermore, HPBW of the antenna is noted to be 69.90, while the SLL is observed to be less than 14.5 dB, as shown in Fig. 3.4.

## 3.2 Design of Aperture Coupled Patch Array

To achieve high-gain for any application, it is suggested to utilize array of the antenna. For specific application, a 1×4 linear patch array is design and presented in this section. Figure 3.5 shows the design of the proposed aperture coupled patch array. Four antenna elements are arranged linearly in the $x$-direction to make 1×4 array, as shown in Fig. 3.5(a). The array occupies an overall size of $W_{S1} \times L_{S1}$ = 96×38.64 mm$^2$. The distance "$d$" between the antenna elements is noted to be 14.75 mm, which is approximately equal to $\lambda_0/2$, where $\lambda_0$ is the free-space wavelength. The distance between the patches tend to reduce coupling between the antenna elements. A typical corporate feeding network is used to excite the array components (see Fig. 3.5b). The design process described in [52] is used to create the corporate feeding network. The parameters $W_{50}$, $W_{70.7}$, and $W_{100}$ corresponds to the line width of 50 Ω, 70.7 Ω, and 100 Ω characteristics impedance, respectively. The rest of the design parameters of the array are listed in Table 3.2.

The parameters listed in Table 3.2 are optimized during the simulation process to achieve better response from the proposed array. One thing needs to be mentioned

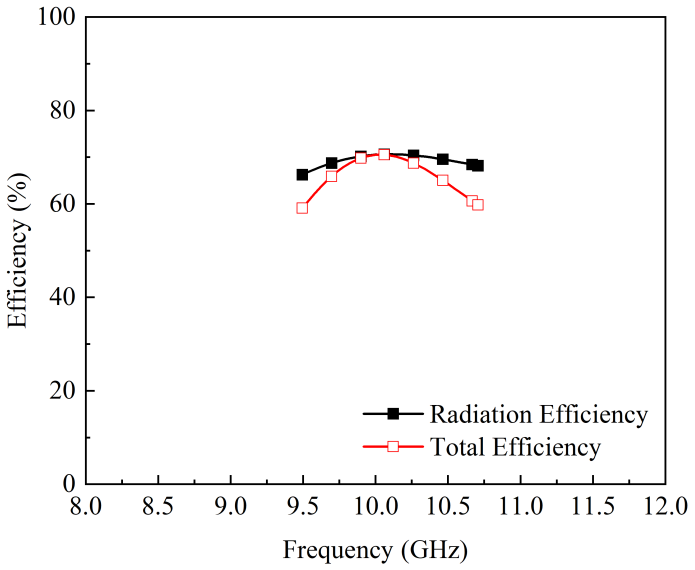


(a)

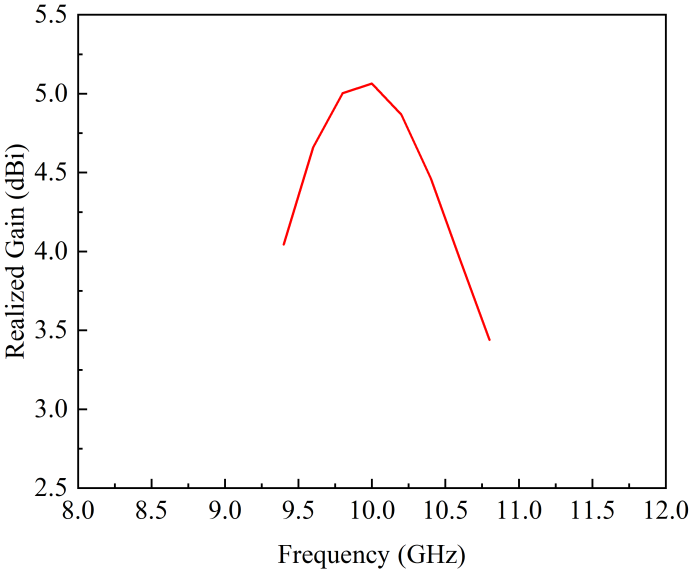


(b)

FIGURE 3.3: Simulated (a) radiation and total efficiency (b) realized gain of the aperture coupled patch antenna.

TABLE 3.2: Design parameters of the aperture coupled patch array antenna (all dimensions in mm).

| $L_F$ | $W_{50}$ | $L_1$ | $L_2$ | $L_3$ | $L_4$ | $W_{70.7}$ | $W_{100}$ | $d$ |
|---|---|---|---|---|---|---|---|---|
| 10 | 2 | 47.68 | 9.5 | 23.68 | 10.6 | 0.8 | 0.32 | 14.75 |

here that the lengths $L_2$ and $L_4$ provide significant effect on the performance of array.

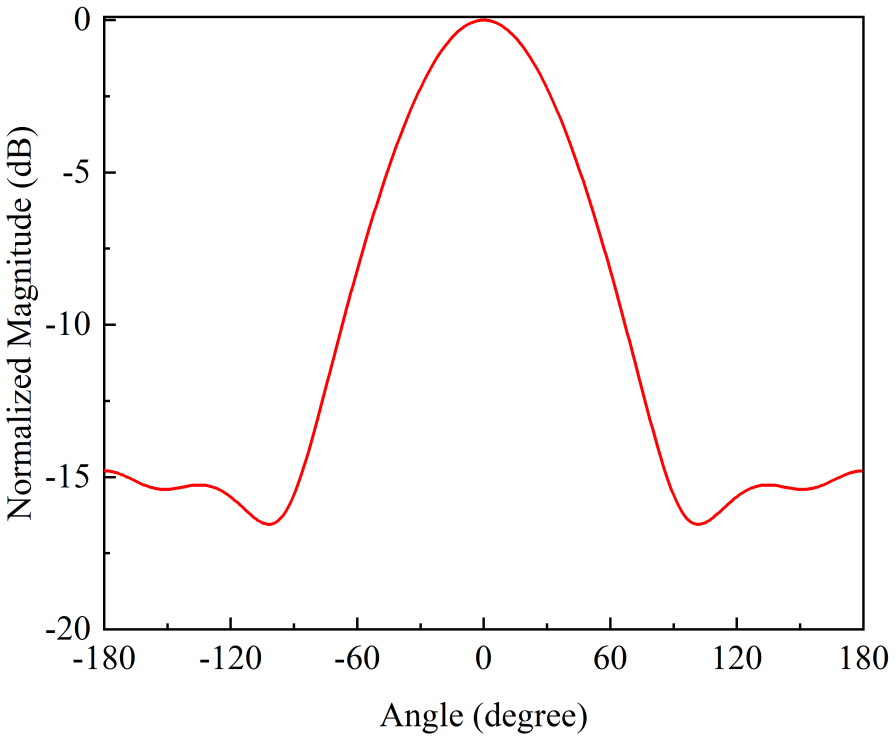


FIGURE 3.4: Simulated far-field H-plane radiation characteristics of aperture coupled patch antenna.

### 3.2.1 Simulation Results

The proposed aperture coupled patch array antenna's simulated $S_{11}$ is depicted in Fig. 3.6. The designed antenna is resonating well in the 10 GHz frequency spectrum. According to the -10 dB bandwidth requirement, the antenna's impedance bandwidth ranges from 9.4 to 10.5 GHz, as illustrated in Fig. 3.6. One can observe from the figure that the proposed array also resonates between 11 and 11.5 GHz, which might be the due to the coupling between the antenna elements.

Figure 3.7 illustrates the realized gain of the array antenna. As observed, the gain of the antenna array increased up to 8.9 dBi in the band of interest and fluctuates in the range of 7.9-8.9 dBi in the operating bandwidth (see Fig. 3.7). The gain in increased up to 3.5 dB by using array configuration.

The normalized far-field H-plane radiation characteristics of the proposed array are shown in Fig. 3.8. The HPBW of the array is noted to be 15.80 with a SLL of -14.5 dB. From the above-presented discussion, it can be observed that the array provides sufficient gain, narrow beamwidth, and reduced SLL in the H-plane.

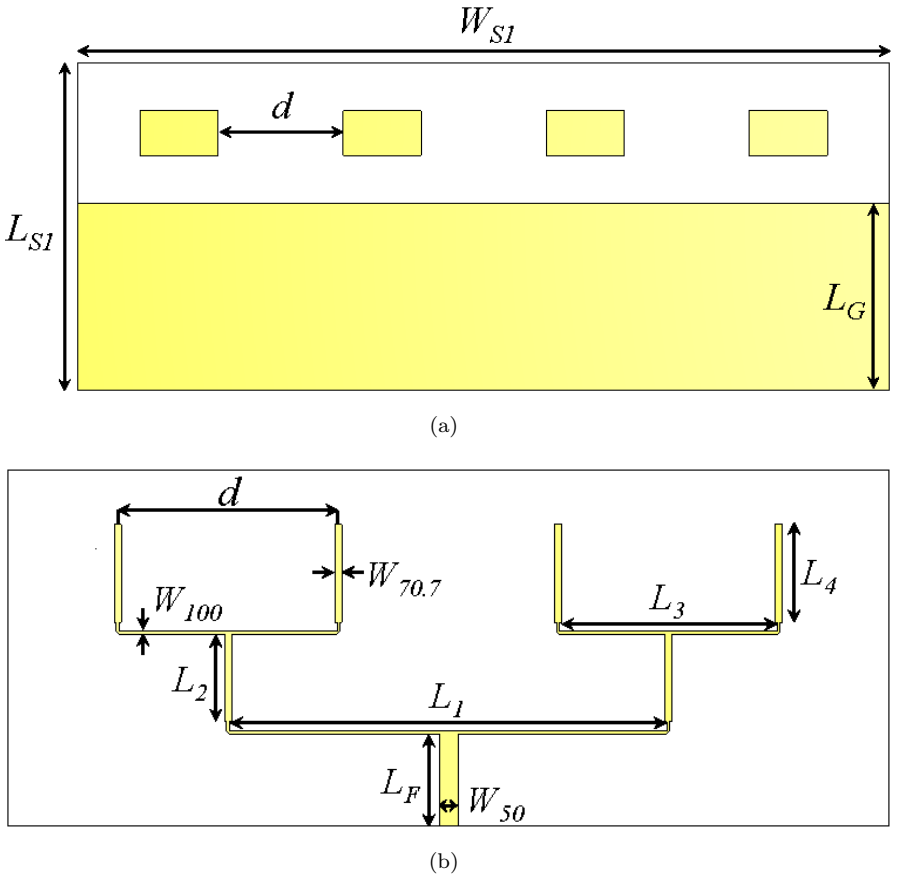


FIGURE 3.5: Design of the proposed 14 aperture coupled patch array (a) patch elements arranged in a linearly (b) corporate feeding network.

For further enhancement in gain and to reduce SLLs, an FSS reflector is designed and placed on the back side of the proposed array, which is shown in Fig. 3.5. The detail about FSS design and the proposed array antenna is provided in the next section.

## 3.3 FSS-based Aperture Coupled Patch Array

### 3.3.1 FSS Design

The proposed FSS unit-cell design is shown in Fig. 3.9. It can be noted from the figure that the FSS unit-cell is composed of a modified square-loop element. A loop-element is selected because it provides wideband response and also offers linear phase response in the band of interest, which is the basic requirement to

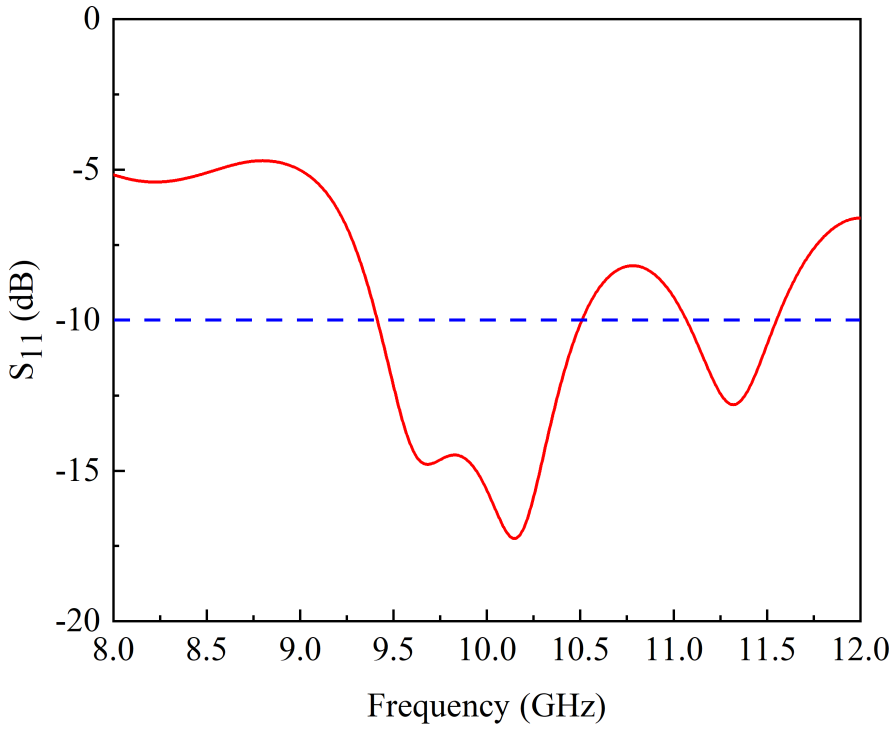


FIGURE 3.6: Simulated $S_{11}$ of aperture coupled patch array antenna.

achieve a high-gain. The design parameters of FSS are optimized during the simulation process to get a response at the 10 GHz frequency band. The parameters are: $W = L = 8.5$ mm, and $W_1 = L_5 = 7.5$ mm. The simulated S-parameters of the proposed FSS are shown in Fig. 3.10. From the figure it is observed that the designed FSS is resonating well for the 10 GHz frequency band. The bandwidth of the FSS according to -10 dB bandwidth criteria is noted to be 4.39 GHz in the frequency range of 8-12.39 GHz, as shown in Fig. 3.10. For high-gain antenna applications, it is required that the FSS should provide linear phase response in the band of interest. Therefore, in Fig. 3.11, the reflection phase response of the proposed FSS is illustrated. One can note that the designed FSS has a linear phase in the band of interest, which shows that the deigned FSS can be utilized as a reflector to improve the gain of an antenna.

### 3.3.2 FSS Integrated Aperture Coupled Patch Array

This section presents the design of the FSS integrated aperture coupled patch array antenna is presented. The geometry of the proposed array antenna is shown

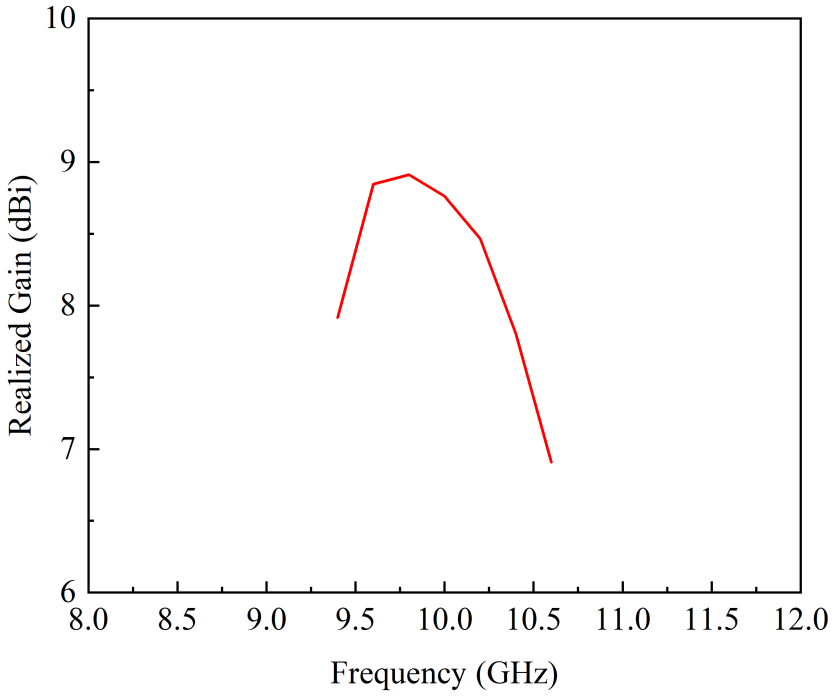


FIGURE 3.7: Simulated realized gain of the aperture coupled patch array antenna.

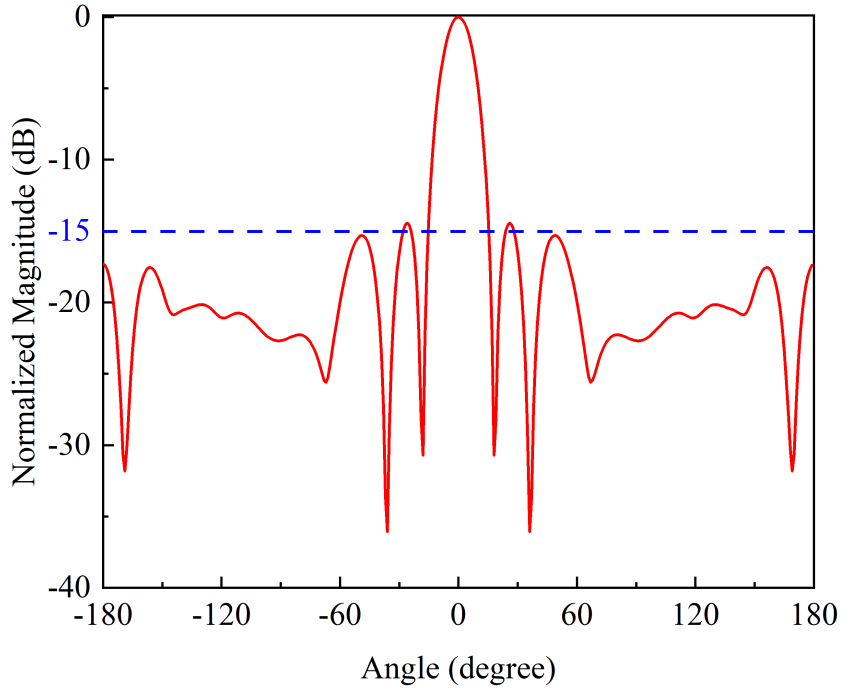


FIGURE 3.8: Simulated H-plane radiation properties of the aperture coupled patch array antenna.

in Fig. 3.12(a, b). The FSS reflector is placed on the back side of the array at a distance of 16 mm, which is approximately equal to $\lambda_0/2$ at the center frequency of 10 GHz, as shown in Fig. 3.12(a). An array of 7×14 unit-cells is designed

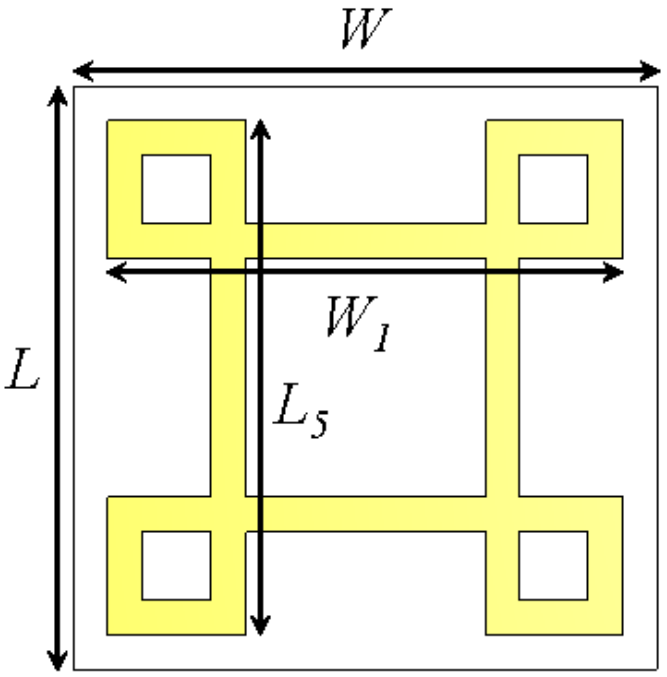


FIGURE 3.9: Design of the proposed FSS unit-cell.

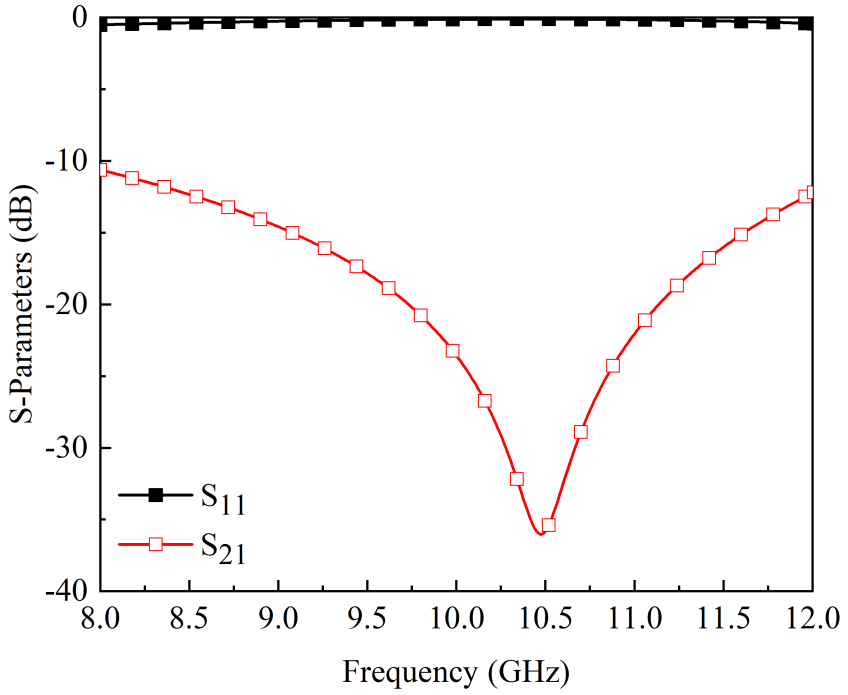


FIGURE 3.10: Simulated S-parameters of the proposed FSS unit-cell.

and used in the proposed configuration, as shown in Fig. 3.12(a). The overall dimensions of the FSS array are noted to be 119×59.5 mm$^2$.

In both the X and Y directions, the distance between unit cells is 1 mm. To get maximum response at the desired resonance frequency and bandwidth, this

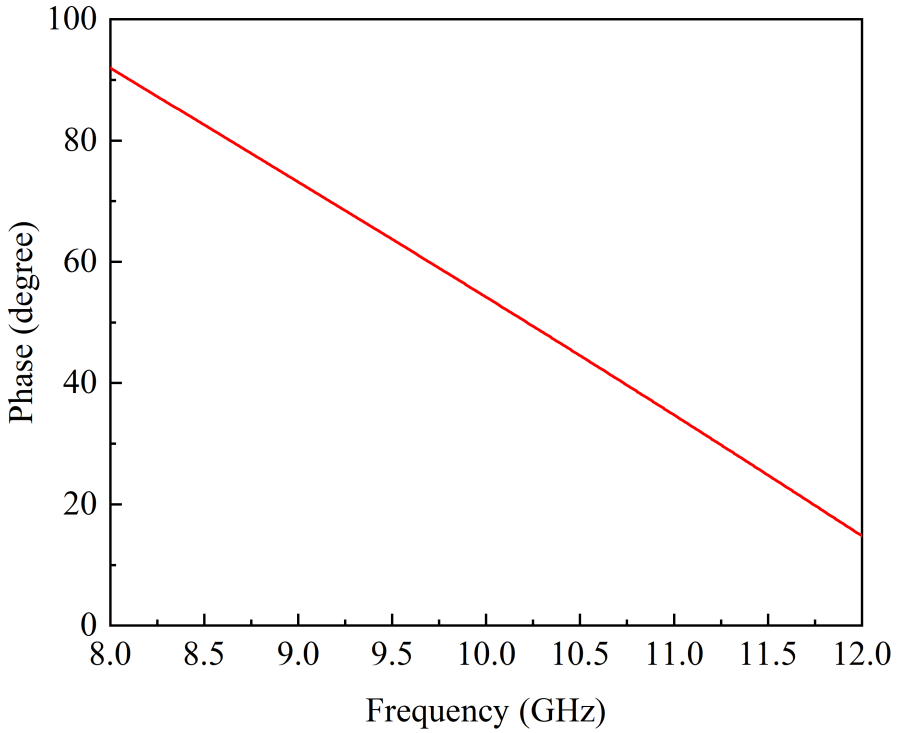


FIGURE 3.11: Simulated reflection phase response of the proposed FSS unit-cell.

spacing is optimized. The resonant frequency and bandwidth of the frequency selective surface are greatly affected by the distance between the unit cells [28]. As spacing is decreased it increases the capacitance between the edges of unit cell and vice versa. The capacitance between the edges of a unit cell increases as distance decreases, and vice versa.

The bandwidth is also affected by the distance between unit cells. If we vary it by 10% in both the X and Y directions, the on the whole bandwidth will change by 20%.

Unit cell spacing has large effect on the mutual coupling. We must make a trade-off between the mutual coupling and the grating lobe in order to achieve the optimal and desired performances. If we choose a lesser spacing, this will increase mutual coupling. If we choose a larger spacing, unfortunately, this will cause grating lobe problem.

The effect of distance between FSS and antenna array on $S_{11}$ and gain is presented in Fig. 3.13. The distance between the FSS and array is changed from 10 mm to

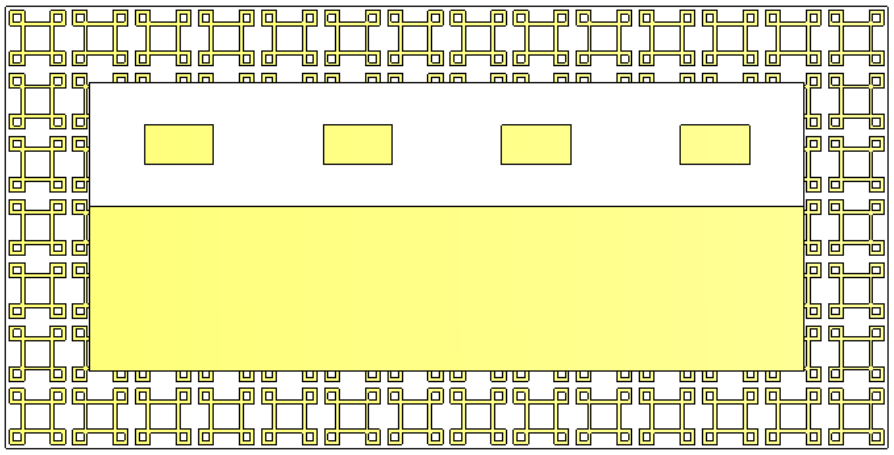

(a)

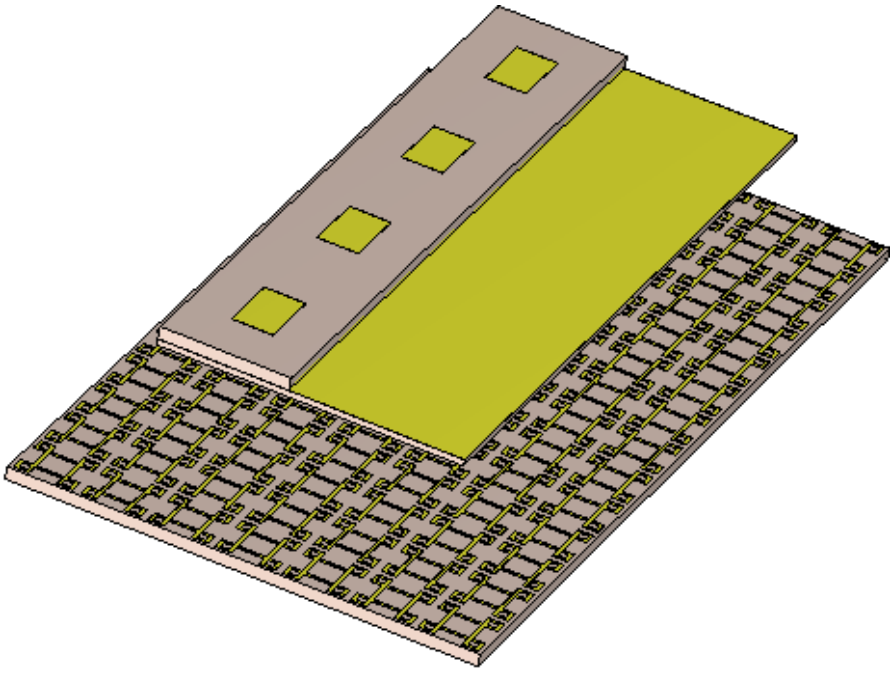

(b)

FIGURE 3.12: Configuration of the proposed FSS integrated aperture coupled patch array (a) front-view (b) perspective-view.

20 mm with a gap of 2 mm. It is observed that for all values of $d_1$, the array is working perfectly for the band of interest, as shown in Fig. 3.13(a).

The maximum impedance bandwidth is noted for $d_1 = 18$ mm, but in this case, the gain of the array is low, as illustrated in Fig. 3.13(b). The acceptable bandwidth and gain value is noted for $d_1 = 16$ mm, and this value is chosen for final antenna array design. The peak gain for the presented case is noted to 11.2 dBi, as shown in Fig. 3.13(b).

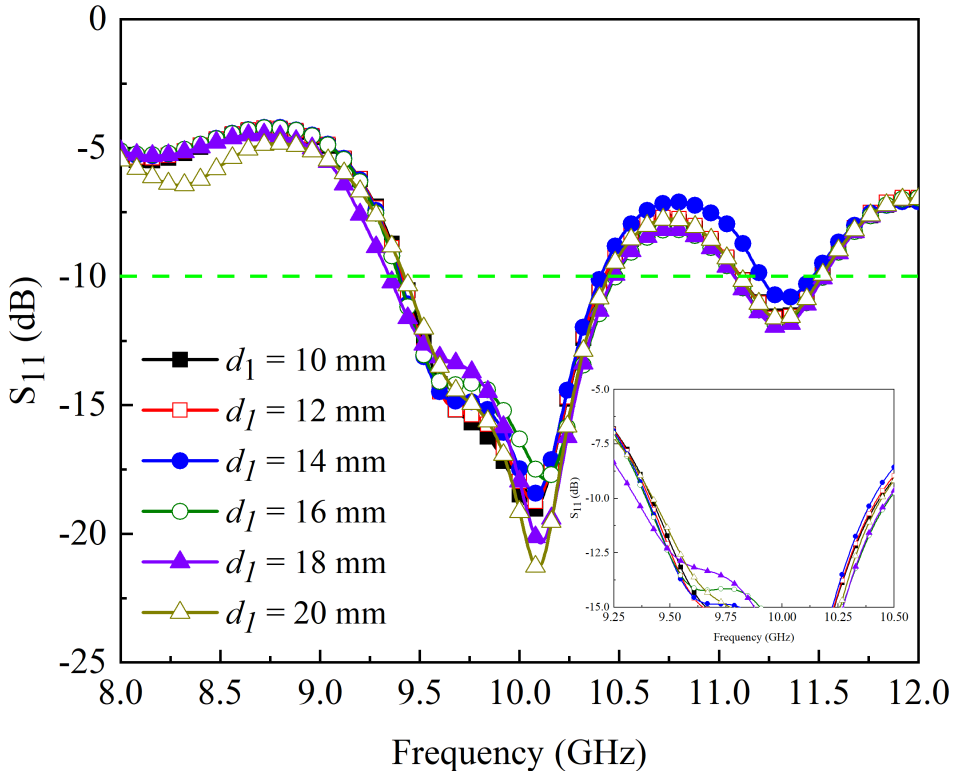


(a)

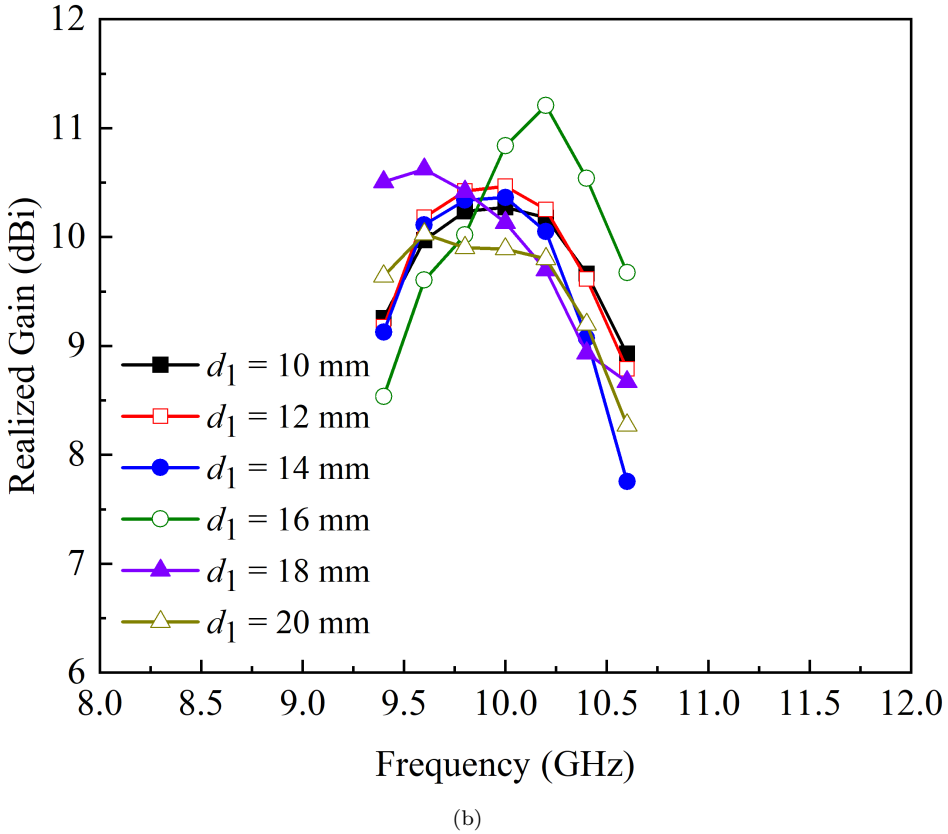


(b)

FIGURE 3.13: Effect of $d_1$ on arrays (a) $S_{11}$ and (b) realized gain.

The $S_{11}$ response of the FSS integrated array is depicted in Fig. 3.14. It is seen that the array is able to provide an impedance bandwidth of 1.09 GHz from 9.39 GHz to 10.48 GHz, which is almost equal to the bandwidth of single antenna element (see Fig. 3.2) and conventional array (see Fig. 3.6).

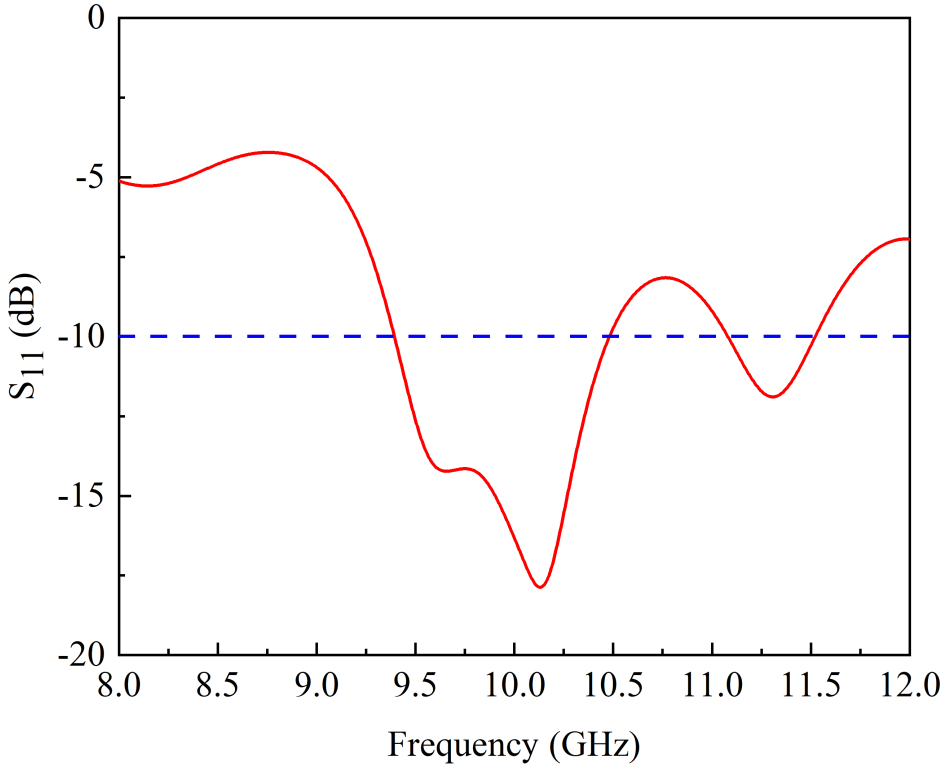


FIGURE 3.14: Simulated $S_{11}$ of the FSS integrated aperture coupled patch array antenna.

The normalized far-field H-plane radiation characteristics of the FSS integrated array antenna are shown in Fig. 3.15. It is observed from the figure that the HPBW of the proposed system is equal to 15.80 with a SLL of -16.7 dB. A comparison between all the proposed designs is listed in Table 3.3. From the data of the table, it can be noted that for all the configurations, the bandwidth is almost equal. Furthermore, the gain of the antenna is increased up to 3.84 dB by utilizing array configuration and it is further increased up to 2.3 dB with the use of FSS reflector. In addition, the SLL of the array is reduced by 2.2 dB by adopting FSS integrated array design. This effect can also be observed from the result of Fig. 3.16 where the H-plane patterns of all the configurations are depicted. As observed, the FSS-based array offers high gain, low SLLs, and narrow beamwidth compared to the other presented configurations.

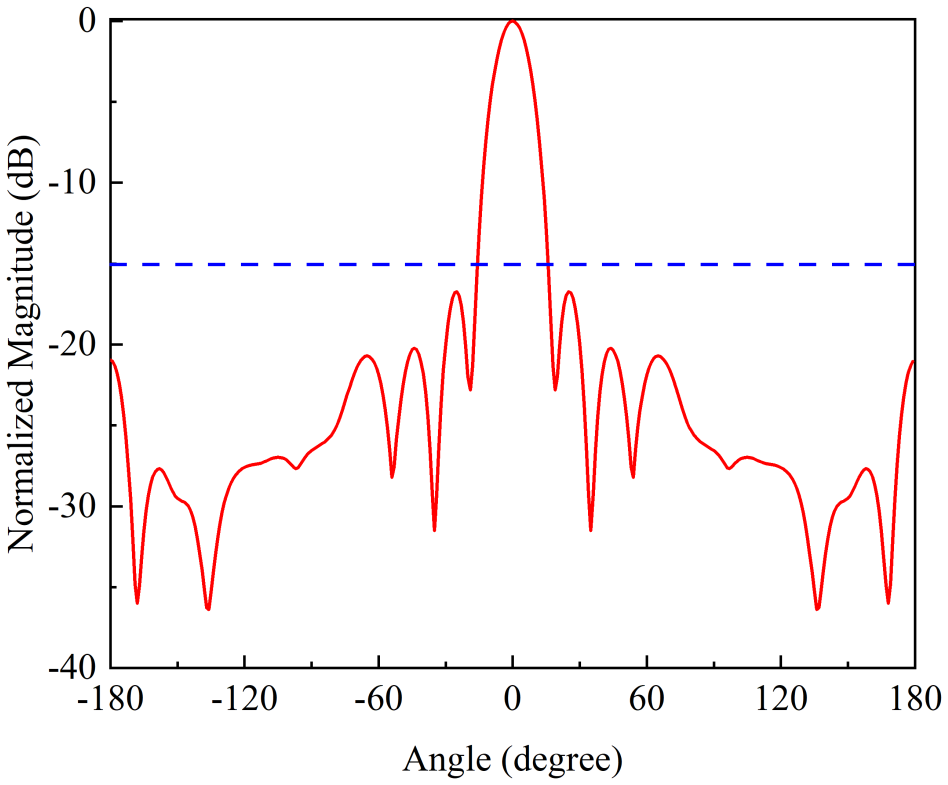


FIGURE 3.15: Simulated H-plane radiation properties of the FSS integrated aperture coupled patch array antenna.

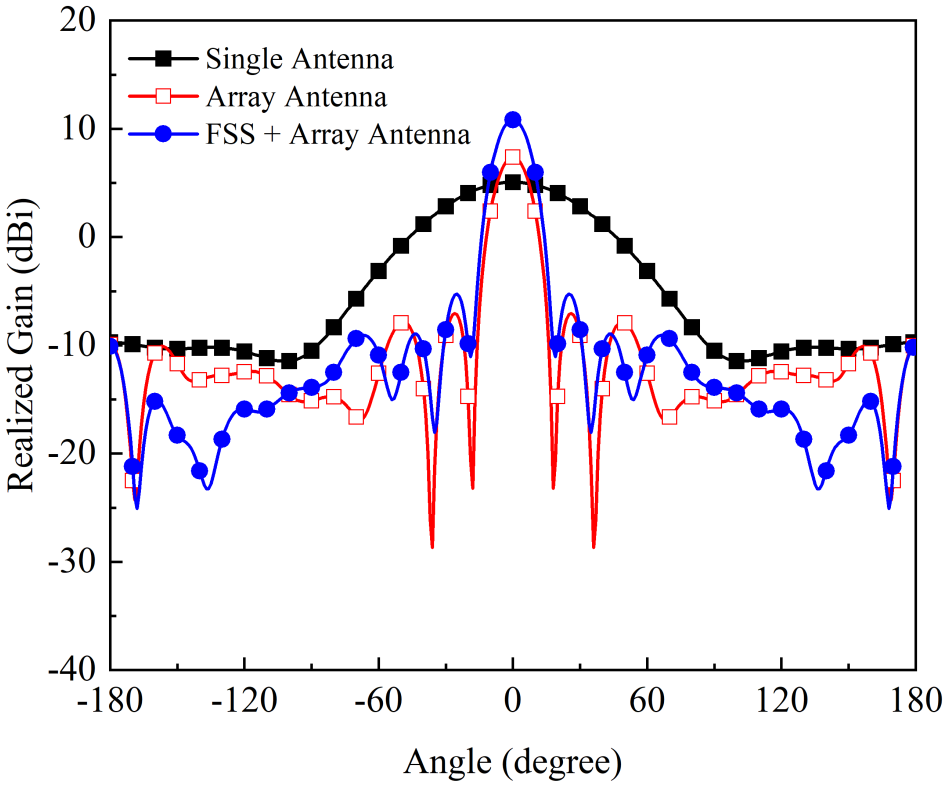


FIGURE 3.16: Comparison between H-plane radiation properties of the proposed antenna configurations.

TABLE 3.3: Performance comparison between the proposed configurations for X-band applications.

| Configuration | Frequency Band (GHz) | Bandwidth (GHz) | Peak Gain (dBi) | Beamwidth (degree) | SLL (dB) | Gain Enhancement (dB) |
|---|---|---|---|---|---|---|
| Single Antenna | 9.52-10.6 | 1.08 | 5.06 | 69.9 | 14.5 | – |
| Array Antenna | 9.4-10.5 | 1.1 | 8.9 | 15.8 | 14.5 | 3.84 |
| Array Antenna with FSS | 9.39-10.48 | 1.09 | 11.2 | 15.8 | 16.7 | 2.3 |

TABLE 3.4: Comparison between proposed and previosuly reported array antennas.

| Ref. | Frequency Band (GHz) | Bandwidth (GHz) | Peak Gain (dBi) | Beamwidth (degree) | SLL (dB) |
|---|---|---|---|---|---|
| [42] | 5.25-6.48 | 1.23 | 11.8 | 32.8 | – |
| [46] | 3.5-5.8 | 2.3 | 12.4 | – | – |
| Proposed | 9.39-10.48 | 1.09 | 11.2 | 15.8 | 16.7 |

A comparison between proposed and previously presented array antennas is provided in Table 3.4. It is noted from the table that the proposed design offers narrow beamwidth compared to the design of [42]. In addition, the performance of the proposed design is almost the same.

## 3.4 Summary

For X-band applications, the design and simulation of an FSS integrated aperture coupled patch array antenna are presented in this chapter. A step-by-step design procedure is provided for the proposed array. In the first step, a single element of aperture coupled patch is designed, which resonates at the 10 GHz frequency band. In the second step, a 1×4 linear array is designed for the desired frequency range in order to produce high gain. A typical 1×4 corporate feeding network is utilized for the feeding of array elements. The results show that the array has good performance in the target band and provides a peak gain of 8.9 dBi with SLLs of

14.5 dB. For further enhancement in gain, an array of FSS is utilized and placed beneath the array antenna. The utilization of FSS reflector tends to achieve 11.2 dBi peak gain for the proposed frequency of interest. It is also observed that the SLL of the array is also reduced up to 2 dB with the use of FSS reflector.

# Chapter 4

# Conclusion and Future Recommendations

## 4.1 Conclusion

In this thesis, an aperture coupled patch array antenna has been designed and analyzed for high-gain satellite communication applications. Before designing an array antenna, a single antenna has been designed and its parameters have been optimized to achieve resonance in the 10 GHz frequency band. After optimizing a single antenna element, the designed antenna is arranged in an array configuration to achieve high gain. A 1×4 linear antenna array has been designed, where each antenna element is fed by utilizing a conventional 1×4 corporate feeding network. For enhanced isolation, the distance between the antenna elements is set to $\lambda_0/2$. From the presented array design, an impedance bandwidth of 1.1 GHz with a peak gain of 8.9 dBi has been observed.

In addition, the SLLs of the designed array are noted to be 14.5 dB. To further enhance the gain, an FSS reflector has been designed and placed at a specific distance. It has been observed that the use of FSS enhanced the gain of a conventional array by 2.3 dB without increasing the size of the array. With the use of an FSS reflector, a peak gain of 11.2 dBi has been observed with SLLs of 16.7

dB. Although it does not affect the beamwidth of the antenna. It is clear from the results that the designed antenna array is a viable option for both current and future satellite communication applications.

## 4.2 Future Recommendations

The presented work can be extended in the following ways:

1. Using high permittivity dielectric substrates helps lower the size of the antenna array.
2. With the use of multi-layer FSS, the gain of the array will be further enhanced.
3. The distance between the FSS reflector and antenna array can be reduced to achieve a more compact size so that it can be integrated into small satellite systems.
4. The tradiational FSS reflector can be replaced with metasurfaces for high-gain applications.

# Bibliography


[1] K.-M. Luk, "The importance of the new developments in antennas for wireless communications," *Proceedings of the IEEE*, vol. 99, no. 12, pp. 2082–2084, 2011.

[2] B. G. Evans, P. T. Thompson, G. E. Corazza, A. Vanelli-Coralli, and E. A. Candreva, "1945–2010: 65 years of satellite history from early visions to latest missions," *Proceedings of the IEEE*, vol. 99, no. 11, pp. 1840–1857, 2011.

[3] R. L. Haupt and Y. Rahmat-Samii, "Antenna array developments: A perspective on the past, present and future," *IEEE Antennas and Propagation Magazine*, vol. 57, no. 1, pp. 86–96, 2015.

[4] Z. Xiao, Z. Han, A. Nallanathan, O. A. Dobre, B. Clerckx, J. Choi, C. He, and W. Tong, "Antenna array enabled space/air/ground communications and networking for 6G," *IEEE Journal on Selected Areas in Communications*, vol. 40, 2022.

[5] I. S. Ammer, M. S. Alsahulli, and A. A. Abd Alkader, "Performance optimization of microstrip patch antenna array for WLAN and LTE 4G technologies."

[6] V. A. Almeida Filho and A. L. P. Campos, "Performance optimization of microstrip antenna array using frequency selective surfaces," *Journal of Microwaves, Optoelectronics and Electromagnetic Applications*, vol. 13, pp. 31–46, 2014.

[7] P. K. Bondyopadhyay, "The first application of array antenna," in *Proceedings 2000 IEEE International Conference on Phased Array Systems and Technology (Cat. No. 00TH8510)*. IEEE, 2000, pp. 29–32.

[8] R. Simons and M. FIEE, "Guglielmo marconi and early systems of wireless," *GEC Review*, vol. 11, no. 1, pp. 37–55, 1996.

[9] C. A. Balanis, *Antenna theory: analysis and design*. John Wiley & Sons, USA, 2015.

[10] H. Gangadhar, "Radiation pattern for broad side array and end fire array antennas," *International Journal of New Technologies in Science and Engineering*, vol. 5, no. 5, pp. 97–105, 2018.

[11] R. A. Abimbola and A. K. Akinwale, "Design and analysis of broadside arrays of uniformly spaced linear elements," *International Journal of Computer Applications*, vol. 975, p. 8887, 2016.

[12] L. Vishalkumar, K. Sandip, and S. S. Kashyap, "Design of planar microstrip patch antenna for GPS application," *European Journal of Academic Essays*, vol. 2, no. 3, pp. 32–36, 2015.

[13] N. H. M. Adnan, I. M. Rafiqul, and A. Z. Alam, "Effects of inter-element spacing and number of elements on planar array antenna characteristics," *Indonesian Journal of Electrical Engineering and Computer Science (IJEECS)*, vol. 10, no. 1, pp. 230–240, 2018.

[14] L. C. Godara, "Applications of antenna arrays to mobile communications. i. Performance improvement, feasibility, and system considerations," *Proceedings of the IEEE*, vol. 85, no. 7, pp. 1031–1060, 1997.

[15] R. Sturdivant, C. Quan, and E. Chang, *Systems Engineering of Phased Arrays*. Artech House, 2018.

[16] A. Dalli, L. Zenkouar, and S. Bri, "Comparison of circular sector and rectangular patch antenna arrays in C-band," *Journal of Electromagnetic Analysis and Applications*, vol. 4, no. 12, pp. 457–467, 2012.

[17] R. Hill, "A practical guide to the design of microstrip antenna arrays," *Microwave Journal*, vol. 44, no. 2, pp. 166–166, 2001.

[18] I. Singh and V. Tripathi, "Microstrip patch antenna and its applications: a survey," *International Journal of Computer Technology and Applications*, vol. 2, no. 5, pp. 1595–1599, 2011.

[19] W. K. Chen, *The electrical engineering handbook*.

[20] R. A. Sainati, *CAD of Microstrip Antennas for Wireless Applications*. USA: Artech House, Inc., 1996.

[21] Z. N. Chen and M. Y. W. Chia, *Broadband planar antennas: design and applications*. John Wiley & Sons, USA, 2006.

[22] D. M. Pozar, "Microstrip antenna aperture-coupled to a microstripline," *Electronics letters*, vol. 21, p. 49, 1985.

[23] S. Targonski, R. Waterhouse, and D. Pozar, "Design of wide-band aperture-stacked patch microstrip antennas," *IEEE Transactions on Antennas and Propagation*, vol. 46, no. 9, pp. 1245–1251, 1998.

[24] D. M. Pozar *et al.*, "A review of aperture coupled microstrip antennas: History, operation, development, and applications," *University of Massachusetts at Amherst*, pp. 1–9, 1996.

[25] Y. Rhazi, S. Bri, and R. Touahani, "Effect of microstrip antenna feeding in the K-band," *International Journal of Engineering and Technology (IJET)*, vol. 4, no. 6, pp. 515–522, 2013.

[26] B. Kamo, S. Cakaj, V. Koliçi, and E. Mulla, "Simulation and measurements of VSWR for microwave communication systems," *Int'l J. of Communications, Network and System Sciences*, vol. 5, no. 11, 2012.

[27] W. L. Stutzman and G. A. Thiele, *Antenna theory and design*. John Wiley & Sons, USA, 2012.

[28] B. A. Munk, *Frequency selective surfaces: theory and design*. John Wiley & Sons, USA, 2005.

[29] H.-Y. Chen and Y. Tao, "Performance improvement of a U-slot patch antenna using a dual-band frequency selective surface with modified Jerusalem cross elements," *IEEE Transactions on Antennas and Propagation*, vol. 59, no. 9, pp. 3482–3486, 2011.

[30] K. Sharma, S. Vaid, and A. Mittal, "An investigation on high-gain dual-polarized cavity reflex antenna using slotted-patch FSS superstrate," in *2013 Fourth International Conference on Computing, Communications and Networking Technologies (ICCCNT)*. IEEE, 2013, pp. 1–4.

[31] K. Sharma and Vaid, "Dual-polarized resonant cavity antenna using slotted-circular patch FSS," in *2013 IEEE International RF and Microwave Conference (RFM)*, 2013, pp. 75–78.

[32] K. Pengthaisong, P. Krachodnok, and R. Wongsan, "Design of a dual-band antenna using a patch and frequency selective surface for WLAN and WiMAX," in *2013 10th International Conference on Electrical Engineering/Electronics, Computer, Telecommunications and Information Technology*. IEEE, 2013, pp. 1–4.

[33] Y. Jia, Y. Liu, and S. Gong, "Low RCS, high-gain and wideband mushroom antenna using frequency selective surface," in *2014 Asia-Pacific Microwave Conference*. IEEE, 2014, pp. 194–196.

[34] F. Meng and S. K. Sharma, "A dual-band high-gain resonant cavity antenna with a single layer superstrate," *IEEE Transactions on Antennas and Propagation*, vol. 63, no. 5, pp. 2320–2325, 2015.

[35] J.-j. Tang, X.-l. Wu, J. Li, X.-y. Li, and Z.-x. Zhang, "A high gain microstrip antenna integrated with the novel FSS," in *2015 4th International Conference on Computer Science and Network Technology (ICCSNT)*, vol. 1. IEEE, 2015, pp. 1182–1185.

[36] X.-y. Li, J. Li, J.-j. Tang, X.-l. Wu, and Z.-x. Zhang, "High gain microstrip antenna design by using FSS superstrate layer," in *2015 4th International*

*Conference on Computer Science and Network Technology (ICCSNT)*, vol. 1. IEEE, 2015, pp. 1186–1189.

[37] N. Muhammad, H. Umair, Z. U. Islam, Z. Khitab, I. Rashid, and F. A. Bhatti, "High gain FSS aperture coupled microstrip patch antenna," *Progress In Electromagnetics Research C*, vol. 64, pp. 21–31, 2016.

[38] S. Shaik and R. P. Dwivedi, "High gain stacked patch antenna with circular polarization for wireless applications," in *2017 International Conference on Nextgen Electronic Technologies: Silicon to Software (ICNETS2)*. IEEE, 2017, pp. 322–326.

[39] A. Kesavan, J. Zaid, and T. A. Denidni, "Wideband FSS superstrate for millimeter-wave antenna gain enhancement," in *2017 IEEE International Symposium on Antennas and Propagation & USNC/URSI National Radio Science Meeting*. IEEE, 2017, pp. 1073–1074.

[40] M. E. Newton, S. Mou, K. Ma, N. Yan, and F. Meng, "A high frequency microstrip patch antenna integrated with FSS using substrate integrated suspended-line technology," in *2018 International Conference on Microwave and Millimeter Wave Technology (ICMMT)*. IEEE, 2018, pp. 1–3.

[41] K. Belabbas, D. Khedrouche, and A. Hocini, "Design and analysis of millimeter-wave microstrip antenna with new FSS superstrate structure," in *2018 International Conference on Applied Smart Systems (ICASS)*. IEEE, 2018, pp. 1–3.

[42] A. Tiwari and S. Das, "FSS loaded high gain antenna array for C-band applications," in *2018 IEEE Indian Conference on Antennas and Propogation (InCAP)*. IEEE, 2018, pp. 1–4.

[43] M. Asaadi, I. Afifi, and A.-R. Sebak, "High gain and wideband high dense dielectric patch antenna using FSS superstrate for millimeter-wave applications," *IEEE Access*, vol. 6, pp. 38 243–38 250, 2018.

[44] M. Asaadi, A. Beltayib, and A. Sebak, "High gain high dense dielectric patch antenna using FSS superstrate for millimeter-wave applications," in *2018 18th International Symposium on Antenna Technology and Applied Electromagnetics (ANTEM)*. IEEE, 2018, pp. 1–2.

[45] G. Srinivas and D. Vakula, "High gain and wide band antenna based on FSS and RIS configuration," *Radioengineering*, vol. 30, no. 1, 2021.

[46] H. Alwareth, I. M. Ibrahim, Z. Zakaria, A. J. A. Al-Gburi, S. Ahmed, and Z. A. Nasser, "A wideband high-gain microstrip array antenna integrated with frequency-selective surface for sub-6 GHz 5G applications," *Micromachines*, vol. 13, no. 8, p. 1215, 2022.

[47] Z. Nassr, S. Zabri, N. Shairi, Z. Zakaria, A. Othman, and A. Zobilah, "Performance improvement of a slotted square patch antenna using FSS superstrate for wireless application," in *Journal of Physics: Conference Series*, vol. 1502, no. 1. IOP Publishing, 2020, p. 012030.

[48] A. Kapoor, R. Mishra, and P. Kumar, "A compact high gain printed antenna with frequency selective surface for 5G wideband applications," *Advanced Electromagnetics*, vol. 10, no. 2, pp. 27–38, 2021.

[49] R. A. Pandhare and M. P. Abegaonkar, "Design of UWB antenna for high gain using FSS reflector," in *2021 IEEE Indian Conference on Antennas and Propagation (InCAP)*. IEEE, 2021, pp. 867–870.

[50] N. O. Parchin, A. Ullah, H. M. Santos, C. H. See, and R. A. Abd-Alhameed, "Gain enhancement of diversity slot antenna using FSS with metamaterial unit cells for UWB systems," in *2022 IEEE Wireless Antenna and Microwave Symposium (WAMS)*. IEEE, 2022, pp. 1–4.

[51] H. A. Mohamed, M. Edries, M. A. Abdelghany, and A. A. Ibrahim, "Millimeter-wave antenna with gain improvement utilizing reflection FSS for 5G networks," *IEEE Access*, vol. 10, pp. 73 601–73 609, 2022.

[52] D. M. Pozar, *Microwave Engineering*. John Wiley & Sons, USA, 2011.